Development and assembly of a sampling device and a dilution system for brake particle measurements in test drives

Bachelorthesis Nr. 1314/18

Editor: Albert Guerra | 2380650
Advisor: Hartmut Niemann, M. Sc.

TECHNISCHE UNIVERSITÄT DARMSTADT

FZD FAHRZEUGTECHNIK TU DARMSTADT

Albert Guerra
Matriculation number: 2380650
Course: Mechanical and Process Engineering

Bachelor Thesis Nr. 1314/18
Topic: Development and assembly of a sampling device and a dilution system for brake particle measurements in test drives

Submitted: 3. September 2018

Technische Universität Darmstadt
Fachgebiet Fahrzeugtechnik
Prof. Dr. rer. nat. Hermann Winner
Otto-Berndt-Straße 2
64287 Darmstadt

Declaration of Authorship

I hereby declare that the thesis submitted is my own unaided work. All direct or indirect sources used are acknowledged as references. This paper was not previously presented to another examination board and has not been published.

Darmstadt, 3. September Se 2018

Abstract

Due to the reduction of exhaust emissions in the last years, the percentage of particulate matter emitted by non-exhaust sources has increased. Brakes play an important role emitting more than half of this type of emissions.[1] The FZD department is carrying a research in order to reach a better understanding of the behavior of brake particle emissions and reduce them. For this purpose, real-drive tests have been conducted in previous works and development of new setups to collect particles must be achieved.

The aim of this Bachelor thesis is to develop concepts for measurements in test drives. It is necessary to minimize losses of particles and take representative samples of particulate matter. With the intention of accomplishing these necessities, a study of aerosol losses has been done. The objective of this study is to optimize aerosol transport through sampling tubes.

Two concepts, a full brake enclosure device and a rim shell device, have been developed and their basic operation system is explained. In the first concept, a full sealed shell around the brake is used to minimize particles losses. This could be think to act in a similar way as the sealed chamber used in dynamometer tests and the results should be similar. For that reason, this concept has been rejected. The second concept tries to reach a realistic behavior of particles taking realistic flow conditions due to the airstream entering to the collecting shell through an air scoop and the interaction of particles with the inner surfaces of the rim. Due to the turbulent regime generated and the limited time to manufacture and assembly the setup, its construction has been discarded.

In the study of transport losses different mechanisms have been studied. These mechanisms are diffusional deposition, gravitational settling deposition in horizontal tubes and inclined tubes and inertial deposition in bends. For each one its efficiency has been calculated for a size range of particles and tube lengths. Furthermore, efficiency has been calculated for a particle transport system similar to one that could be used in a test car. With this study, a general approach to the magnitude of transport efficiency has been reached. It has been possible to conclude that losses are much higher for large particles than for small particles. Finally, some considerations to optimize the transport of particles have been presented.

[1] Grigoratos, T.; Martini, G.: Brake wear particle emissions (2015), p.2491.

Table of content

Declaration of Authorship 2
Abstract III
Table of content IV
Symbol and index directory VI
List of abbreviation VII
List of figures VIII
List of tables IX
1 Introduction 1
1.1 Motivation 1
1.2 Concretion of assignment 2
1.3 Methodology 3
2 Background 4
2.1 Aerosol particles in brake cars 4
2.1.1 Dynamometer 4
2.1.2 Tribometer 5
2.1.3 Real-drive 6
2.2 Aerosol measurement instruments 7
2.2.1 Optical Particle Sizer (OPS) / Optical Particle Counter (OPC) 7
2.2.2 Condensation Particle Counter (CPC) 8
2.2.3 Aerodynamic Particle Size (APS) 9
2.2.4 Impactors 9
2.2.5 Other methods 10
2.3 Aerosol losses 11
2.3.1 Sampling losses 11
2.3.2 Transport losses 12
2.3.2.1 Diffusional deposition 12
2.3.2.2 Gravitational settling deposition or sedimentation 12
2.3.2.3 Inertial deposition in bends and constrictions 12
2.3.2.4 Other deposition mechanisms 13
3 Concepts for measurements in test drives 14
3.1 Analysis of requirements 14
3.2 Full brake enclosure device 14
3.3 Rim shell device 16
3.4 Conclusions 18
4 Study of aerosol transport losses 19
4.1 Particles size range 21
4.2 Theoretical losses 21
4.2.1 Diffusional deposition efficiency 21

4.2.2 Gravitational settling deposition efficiency 22
4.2.2.1 Horizontal tubes 22
4.2.2.2 Inclined tubes 23
4.2.3 Inertial deposition efficiency in bends 24
4.2.4 Vehicle test transport system efficiency 25
4.3 Results 26
4.3.1 Diffusional deposition losses 27
4.3.2 Gravitational settling deposition losses 28
4.3.2.1 Horizontal tubes 28
4.3.2.2 Inclined tubes 30
4.3.3 Inertial deposition losses in bends 31
4.3.4 Test vehicle transport system 33
5 Overall conclusions 35
Bibliography 36

Symbol and index directory

Latin letters:

symbol	unit	description
A	mm^2	area
C_C	-	Cunningham slip correction factor
D	m^2/s	particle diffusion coefficient
d	m	diameter
d_p	m	particle diameter
g	m/s^2	gravitational acceleration
k	N·m/k	Boltzmann constant
L	m	length
Q	m^3/s	flow rate
Re	-	Reynolds number
Sh	-	Sherwood number
Stk	-	Stokes number
T	K	temperature
U	m/s	fluid velocity
V_{ts}	m/s	terminal settling velocity

Greek letters:

symbol	unit	description
η	%	efficiency
φ	º, rad	angle of the bend
θ	º	angle of inclination
η	Pa·s	viscosity
μ	Pa·s	dynamic viscosity
ρ	kg/m^3	density
λ	m	mean free path
τ	s	particle relaxation time

List of abbreviation

FZD	Fahrzeugtechnik Darmstadt
TUD	Technische Universität Darmstadt
OPS	Optical Particle Sizer
OPC	Optical Particle Counter
CPC	Condensation Particle Counter
APS	Aerodynamic Particle Sizer
DMA	Differential Mobility Analyzer

List of figures

Figure 1.1: Aerosol causations and correlation 1
Figure 1.2: Procedure points for enclosure concepts 3
Figure 1.3: Procedure method for the study of aerosol transport losses 3
Figure 2.1: Basic components of a dynamometer 4
Figure 2.2: Basic setup of a pin-on-disc machine 5
Figure 2.3: Setup of the real-drive tests by Walhström and Olofsson 6
Figure 2.4: Schematic operation principle of an OPS/OPC 7
Figure 2.5: Schematic operation principle of a CPC 8
Figure 2.6: Schematic operation principle of an APS 9
Figure 2.7: Schematic operation principle of single impactor 10
Figure 2.8: Streamlines in isoaxial sampling 11
Figure 2.9: Summary of transport losses 12
Figure 3.1: Schematic operation principle of the full brake enclosure device system 14
Figure 3.2: Full brake enclosure device concept 15
Figure 3.3: Schematic operation principle of the rim shell device concept 16
Figure 3.4: Rim shell device functioning 16
Figure 3.5: Trajectory of particles through the rim 17
Figure 4.1: Sketch of the particles transport system 25
Figure 4.2: Graphic of fine/coarse particles losses relation 26
Figure 4.3: Graphic of diffusional deposition efficiency (Fine particles) 27
Figure 4.4: Graphic of diffusional deposition efficiency (Coarse particles) 27
Figure 4.5: Graphic of gravitational deposition efficiency in horizontal tubes (Fine particles) 28
Figure 4.6: Graphic of gravitational deposition efficiency in horizontal tubes (Coarse particles) 29
Figure 4.7: Graphic of gravitational deposition efficiency in inclined tubes (Fine particles) 30
Figure 4.8: Graphic of gravitational deposition efficiency in inclined tubes (Coarse particles) 30
Figure 4.9: Graphic of inertial deposition efficiency in bends (Fine particles) 31
Figure 4.10: Graphic of inertial deposition efficiency in bends (Coarse particles) 32
Figure 4.11: Graphic of test vehicle transport system (Fine particles) 33
Figure 4.12: Graphic of test vehicle transport system (Coarse particles) 33

List of tables

Table 4.1: DEHS properties 19
Table 4.2: Air properties 19
Table 4.3: Summary of parameters used in the study 20
Table 4.4: Characteristics of the transport system 25
Table 4.5: Table of efficiency in test vehicle transport system 34

1 Introduction

The emission of particulate pollutants to the atmosphere from cars is one of the topics under investigation in the automotive sector. A correlation between air pollution and a significant increase of diseases and mortality in the population, especially in large cities, make us think about the direct impact of aerosol particles emitted by cars in the human health.

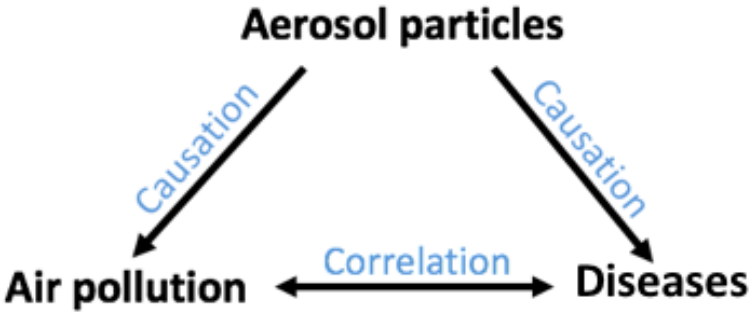

Figure 1.1: Aerosol causations and correlation

Vehicles emit two types of particles: exhaust and non-exhaust particles. Exhaust particles come from petrol and lubricants which have not been burnt by combustion engines. In the last decades, exhaust emissions have been reduced due to the application of laws and regulations by different state and international organizations while other particles emitted from vehicles have not received attention. Furthermore, the automotive industry is evolving to hybrid and electric vehicles, therefore the emission of exhaust particles will continue decreasing in the further years. This means that the percentage of non-exhaust particles in relation to the total mass emissions will increase. These types of particles proceed from non-exhaust sources such as the contact between tyre and road, brakes, or road dust resuspension. Some studies have reported that brake wear can contribute up to 55% by mass to total non-exhaust traffic emissions and up to 21% by mass to total traffic emissions.[2] For these reasons, some commissions and agencies are working to establish regulations to reduce non-exhaust emissions. Hence, it is essential to reach a better understanding of brake wear particles during and after braking events in order to find appropriate solutions. That is why the key concept of this approach is to study the behaviour of brake wear particles under realistic conditions.

1.1 Motivation

Brakes are one of the most important security element of the vehicle. They are used to slow down or stop the movement of the vehicle by transforming the kinetic energy of the car into heat which is dissipated by convection to ambient air, by conduction to cooler components of the brake and by radiation to the environment. Disc brakes have better performance in comparison with drum brakes. Accordingly, current cars use disc brakes instead of drum brakes, at least in the front axle considering

[2] Grigoratos, T.; Martini, G.: Brake wear particle emissions (2015), p.2491.

that front brakes have to apply more than half of the brake effort due to the inertia of motion of the car which shifts the mass to the front part of the vehicle. When the driver hits the brake pedal there is a frictional contact between the disc and the pad. This contact produces the formation of particles of different sizes. It has been reported in some studies that approximately 50% of these particles lie into diameters smaller than 20 μm, 40% of brake wear is emitted as PM_{10} and the rest may deposit on the road surface or vehicle.[3]

Unlike drum brakes, disc brakes are not enclosed in a housing drum, therefore a bigger percentage of the particles produced during braking are emitted to the atmosphere becoming airborne. Different tests have been carried out in laboratory and in the test track so as to characterize the behaviour of that emissions during braking. Söderberg et al.[4] conducted tests of disc brake material in a pin-on-disc machine. Wahlström et al.[5] tested different brake pads in a disc brake assembly test stand and, in addition, conducted a series of field tests using a modern passenger car. These tests will be explained with more detail in the Chapter 2. There have been more tests conducted by other researchers.

For the above reasons, the motivation of this Bachelor thesis is to continue with the study of brake wear emissions in the FZD department of TUD by developing a concept which allows the achievement of trusty results in real test drives and studying losses in aerosol transport with the purpose of optimizing the sampling systems. That would mean a step forward in the research of this kind of emissions with the objective of understanding the behaviour of this particles and reaching a necessary optimization to reduce them.

1.2 Concretion of assignment

The concrete assignment of this Bachelor thesis is to develop solution approaches and select an appropriate concept of a sampling device and a dilution system for brake particle measurements in real test drives.

For the designing of the disc brake enclosing device, the following aspects must be taken with special respect:

- Minimizing losses of particle number: by approaching to the best model to take particle samples out of the brake.
- Particle size independent sampling efficiency
- Create realistic conditions in the disc brake enclosing in order to get realistic samples of wear particles

The assembly and initial setup of the sampling and dilution devices were also part of the project. As well as the verification of the sampling and dilution devices by developing appropriate test drives.

[3] Grigoratos, T.; Martini, G.: Brake wear particle emissions (2015), p.2493.

[4] Söderberg, A. et al.: A Pin on Disc Simulation (2008).

[5] Wahlström, J. et al.: Airborne wear particles from passenger car disc brakes (2010).

Due to technical and timing reasons during the development of this Bachelor thesis the construction of the enclosure device has not been possible.

In addition to the development of collecting devices concepts, a study of the losses in aerosol sampling transportation is also part of the project. With this study, it is intended to optimize the transport of particulate matter from the sampling point to the aerosol measurement device. In order to carry out this study, an aerosol generator and an optical particle sizer device have been used, however, due to the failure of the sensor device the study has been limited to theoretical losses.

1.3 Methodology

This point gives an explanation of the methodology used to develop this project. The final goal of using a structured procedure is to ensure that the objectives of the project will be accomplished. The methodology used to develop the concepts of the disc brake enclosing devices is based on four points, which are: analysis, research, implementation and validation.

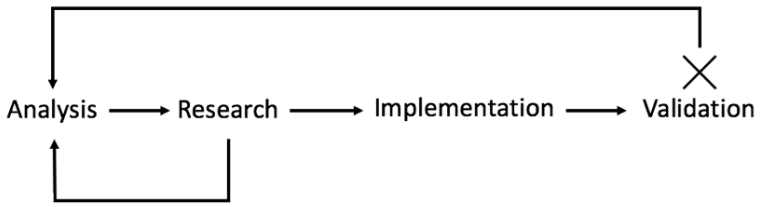

Figure 1.2: Procedure points for enclosure concepts

As the first step, it is necessary to analyze the requirements which must be fulfilled to develop the enclosing devices. Once these requirements are known, the best solution for each one has to be found. The next step is to implement the adopted solution to the concept and finally validate it. If it is not validated, the approach is changed and the research for another solution starts again. To do that, morphological analysis has been used. First, critical problems are detected and then different solutions for each problem are identified. It allows us to eliminate illogical solution combinations. To perform the study of the losses in aerosol sampling transportation a theoretical calculation has been done.

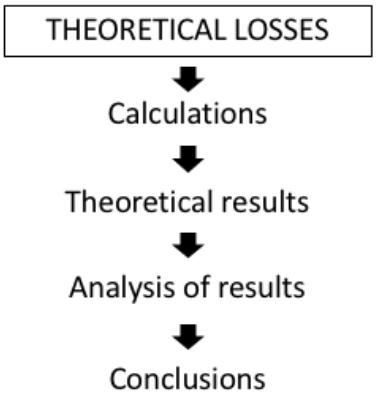

Figure 1.3: Procedure method for the study of aerosol transport losses

2 Background

In this chapter, a theoretical revision of already carried research projects in the study of brake wear particle emissions is presented. Furthermore, an overview of the most commonly used methods to measure aerosol particles is provided in order to understand the basic operation principles of some of the particle counter devices that are used to perform tests. Finally, the different types of losses in the transport of aerosol are explained in the last point of this chapter.

2.1 Aerosol particles in brake cars

In the field of brake wear particle emissions several studies have been documented by some researchers. All of them have the objective of understanding better what is occurring when contact between the pad and the disc is produced. However, different setups to collect and measure brake particles have been used. They are the dynamometer, the tribometer and real-drive.

2.1.1 Dynamometer

This setup consists of a brake system (disc, pads and caliper) which is connected to an electric motor by a shaft. In most of the setups, an inertia section is also used to simulate the vehicle inertia. These are the basic elements of a dynamometer although some modifications can be found amongst different configurations.

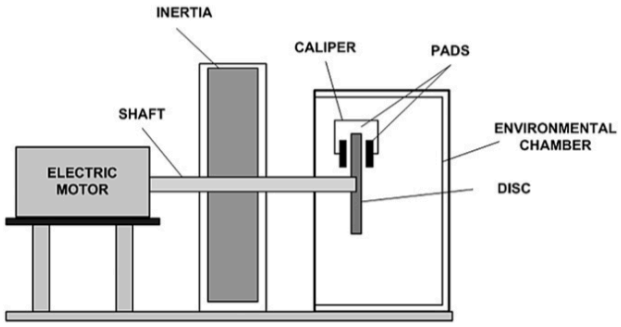

Figure 2.1: Basic components of a dynamometer [6]

The inertia dynamometer shown in the Figure 2.1 has a close environmental chamber around the brake system. Other researches such as Walhström et al.[7], Sanders et al.[8] and Augsburg et al.[9] also have used this enclosure system to reduce particle losses and prevent external contamination from the ambient air. Nonetheless, different solutions have been adopted to collect particles from the sealed chamber. Augsburg et al. used a sample collection tube placed centrally at the end of the measuring

[6] Kukutschová, J. et al.: On airborne nano/micro-sized wear particles (2011), p.999.

[7] Wahlström, J. et al.: A disc brake test stand (2009).

[8] Sanders, P. G. et al.: Brake Dynamometer Measurement (2002).

[9] Augsburg, K. et al.: Measuring and characterization of brake dust particles (2017).

duct to ensure a high efficiency of evacuation and uniformity. Sachse and Augsburg[10], for their part, used a collecting container placed tangentially to the brake caliper to conduct qualitative comparisons of brake dust emission of different brake pad characteristics. Sachse and Augsburg also performed other tests with a closed collecting capsule with air-ventilation for counting the total particle number.

The airflow around the brake system tested in a dynamometer differs from the airflow around the brake in a real car because it is complicated to reproduce it in a laboratory test stand. For this reason, quantitative measurements of airborne particles are uncertain since it is not known what quantity of particles escapes from the vehicle. However, due to the control of the cleanness of the air, qualitative results in relation to size distribution can be obtained using dynamometers.

Sanders et al., apart from performing tests with an enclosed dynamometer, also included a vehicle wheel on the setup in order to simulate the airflow around the brake on a vehicle. Large fraction of wear particles collects on the wheel itself and the total mass collected was reduced by 20%. Furthermore, the airborne mass was reduced from 6 to 3,9 gr. With these observations can be concluded that the components arounds the brake system influence the quantity of airborne wear particles emitted.

2.1.2 Tribometer

With a tribometer, measurements of friction and wear of brake pads and discs can be done. There exist different types of tribometers but, in the field of brake particle emissions, pin-on-disc machines with a rotating disc are used to perform tests.

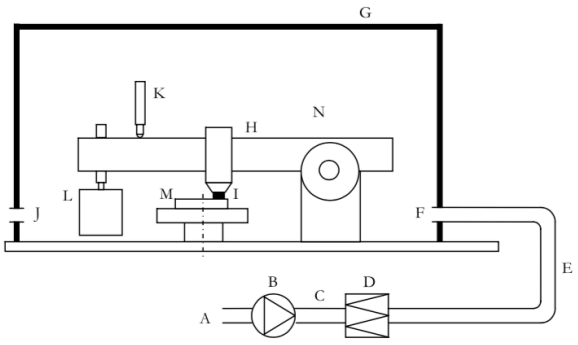

Figure 2.2: Basic setup of a pin-on-disc machine[11]

In the Figure 2.2 the basic structure of a pin-on-disc machine is shown. A dead weight (L) press the pin (I) to the disc (M). Clean air is introduced to the chamber (G) through an inlet (F). To be sure that the air is clean, an HEPA filter (D) is placed after the fan (B). In the outlet (J), a sample point to measure particles is located.

Söderberg et al.[12] reported that the air is well mixed due to the complicated volume of the pin-on-disc machine and the high air change rate being verified by the smooth concentrations measured during the tests. The pins used during the tests had a diameter of 10 mm and a height of 15-17 mm. They

[10] Sachse, H.; Augsburg, K.: Study on Appropriate Measurement Methods (2015).

[11] Söderberg, A. et al.: A Pin on Disc Simulation (2008), p.8.

[12] Söderberg, A. et al.: A Pin on Disc Simulation (2008), p.9.

found a peak at a particle size about 0,3 and 3 µm for number distribution and volume distribution, respectively.

Other studies have been carried out using a microscopy to analyze the surface state of brake pads after applying some brake forces. In addition, tests with transparent brake disc material (borosilicate glass) have been performed to study patch dynamics.

The pin-on-disc machine setup has proven to be useful to measure size distribution and study tribo-layer in pads and discs. However, the total number of particles cannot be read because of the round shape of the pins which is different from the brake pads. Therefore, with this setup qualitative results can be obtained instead of quantitative.

2.1.3 Real-drive

The last method consists of measuring particles directly in real test drives by installing a setup, to collect and transport particles to the measurement devices, in the vehicle. The main advantage when testing in real cars is that the airflow conditions around the brake are realistic. In addition, vehicle components, such as the wheel, can reduce the quantity of airborne particles since they provide a surface where particles can deposit. However, the cleanness of the surrounding air of the brake is difficult to control without influencing on the flow conditions and particles from other sources can have an impact on the results. Due to these difficulties, not so many tests have been carried out in real drives as in dynamometer test stands.

Walhström and Olofsson[13] used two tubes which were mounted between the pad carrier and the shield as can be seen in the Figure 2.3. They also used two tubes at the front of the car to compare concentrations measured at this point and near the brake to determine if the peaks in particle concentration could be related to braking events. Even though the air flow around the brake is different in real-drive, they found a correlation between the results conducted in test stands and the shape of the measured number distribution. They found maximum distribution peaks at approximately 0,35 µm.

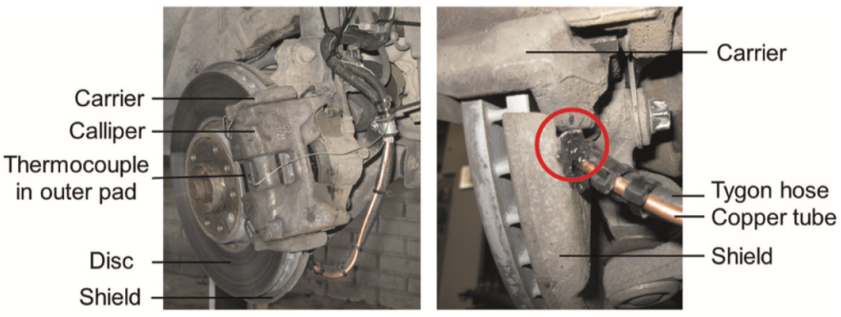

Figure 2.3: Setup of the real-drive tests by Walhström and Olofsson

Sanders et al.[14] also conducted tests on a high-speed track and on public roads. Three stainless steel tubes were connected surrounding the right front wheel. One tube was installed inside the rim and the

[13] Wahlström, J.; Olofsson, U.: A field study of airborne particle emissions (2015).

[14] Sanders, P. G. et al.: Airborne Brake Wear Debris (2003).

other two were positioned outside. An additional tube was mounted next to the caliper. The same setup was also tested in a wind tunnel.

Mathissen et al.[15], performed tests to study ultrafine particle generation with a vehicle equipped with five stainless steel tubes inside the front right wheel housing. During his research, not only studied brake wear debris, but also particles generated from tire-road interface. Near the brake disc the size distribution was found to be unimodal with a maximum peak at approximately 11 nm.

2.2 Aerosol measurement instruments

In this section, a description of the basic principles of operation of some aerosol measurement devices is provided. Aerosol measurement techniques can be classified in two groups: real-time and laboratory analysis. Just real-time techniques will be reviewed since they are directly related with the foreground of this Bachelor thesis of measuring particle brake emissions in real-drives. The most common devices are the Optical Particle Sizers/Counters (OPS/OPC), the Condensation Particle Counter (CPC), the Aerodynamic Particle Sizer (APS) and the Impactors among other methods.

2.2.1 Optical Particle Sizer (OPS) / Optical Particle Counter (OPC)

The OPS/OPC are two of the most used devices for real-time aerosol measurements. They are based on the light scattering principle. A light source, usually a laser beam, is used and when a sample flow of particles enters to the optical chamber and crosses the beam some light is scattered. A parabolic mirror with a wide angle collects the light and directs it onto a photodetector. By counting the number of pulses which the photodetector reads it is possible to count the number of particles in the OPCs. Consequently, the particle number concentration is known. In addition, particle size can be determined by measuring the intensity of the scattered light in the OPSs devices.

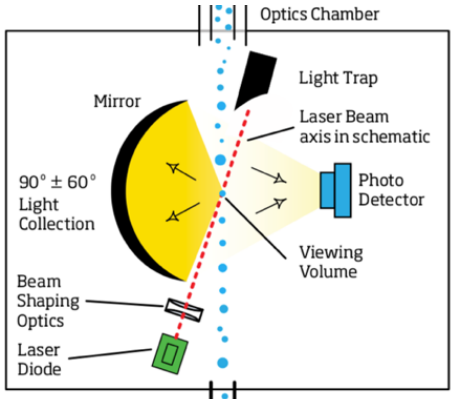

Figure 2.4: Schematic operation principle of an OPS/OPC[16]

In order to measure smaller particles, intensity of the light and sensitivity of the detector must be increased. To achieve a major light intensity, most types of laser operate within a laser cavity. It

[15] Mathissen, M. et al.: Investigation on the potential generation of ultrafine particles (2011).

[16] TSI Incorporated Ltd: Model 3330 (2012), p.2.

consists of using two high reflective mirrors, one at each end of the cavity with the laser between them. The light is retained in the cavity and this stimulates the emission of more light.[17]

In this type of measurement devices, the typical size range of particles starts, in general, from 0.3 µm up to 10-20 µm depending on the model.

2.2.2 Condensation Particle Counter (CPC)

CPCs are used to count particles down to nanometer size range. The principle of laser scattering is also used as in the optical particle counters but the difference is that in CPCs the particles are grown by condensation before being detected by the sensor.

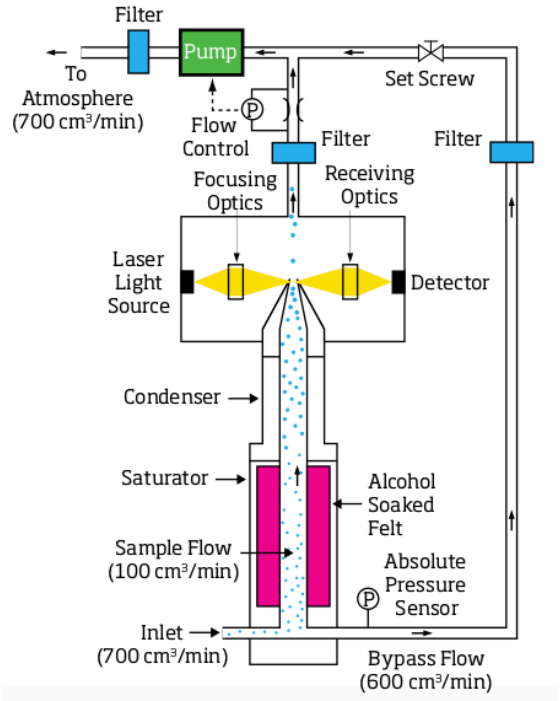

Figure 2.5: Schematic operation principle of a CPC[18]

As in the manual of the CPC Model 3007[19] is explained, this kind of instruments operate by drawing an aerosol sample continuously through a heated saturator, in which alcohol is vaporized and diffuses into the sample stream. Both, aerosol sample and alcohol vapor, pass into a cooled condenser where the alcohol becomes supersaturated and condenses onto particles growing quickly into larger alcohol droplets of µm range. These droplets then are counted by an optical detector and particle number concentration can be determined.

The minimum particle size range detectable by CPCs depends on the difference of temperature between saturator and condenser. Generally, the range goes from some nanometers up to ~1µm.

[17] The University of Manchester: Optical Particle Counters.

[18] TSI Incorporated Ltd: Model 3007 (2012), p.2.

[19] TSI Incorporated Ltd: Model 3007 (2012).

2.2.3 Aerodynamic Particle Size (APS)

The concept of aerodynamic diameter is used to characterize aerosol particles which have irregular shapes. It is defined as the diameter of a standard-density sphere (ρ_o= 1000 kg/m^3) that has the same gravitational settling velocity as the particle in question.[20]

The principle of inertia is used by the APS to size particles. The APS Model 3321 from TSI uses this method and it is explained in its manual[21]: the APS accelerates the aerosol sample flow through a nozzle. As particles exit the nozzle, they cross through two partially overlapping laser beams. Light is scattered and collected by an elliptical mirror, placed at 90 degrees to the laser beam axis, which focuses it onto a photodetector. It converts the light pulses into electrical pulses. Each particle passing through both laser beams produces two pulses. The particle size is determined by the time-of-flight (delay between the pulse) measured.

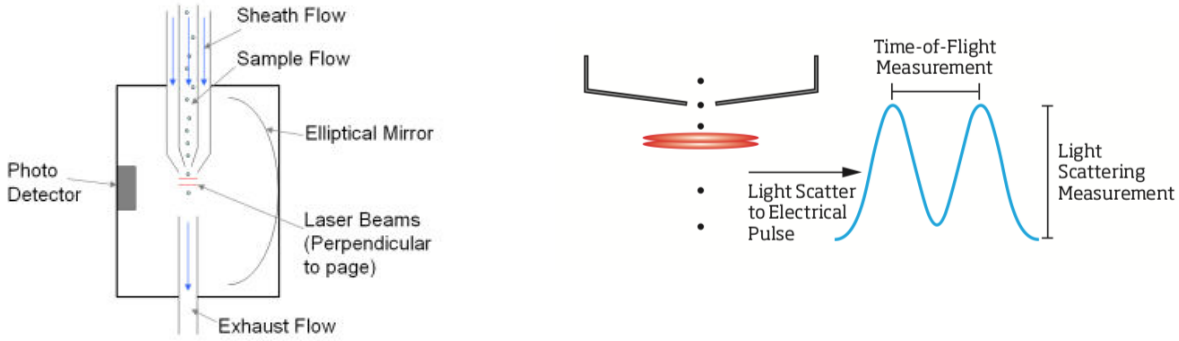

Figure 2.6: Schematic operation principle of an APS[22]

The particle size distribution range that APSs can read goes from 0.5 to 20 μm. It is to say that if only one pulse or more than two pulses are read, they are not used to calculate aerodynamic size. In the former case, it could mean that the particle is too small and skip the second beam or is moving too slowly (very large particles), while in the latter case the reason could be the coincidence of two particles.

2.2.4 Impactors

The inertial impaction is the mechanism used in impactors. This principle is based on the tendency of particles to continue traveling in the initial direction when airstream is forced to change the direction. This is a separation process since the sample flow is accelerated through a nozzle towards a plate situated below. Particles which are small enough will follow the stream lines, while the rest will be deposited or impact on the plate. The size as the particles are collected with 50% efficiency is the cutoff point of impactors.[23]

[20] Baron, P. A. et al.: Aerosol measurement (2011), p.24.

[21] TSI Incorporated Ltd: Model 3321 (2004).

[22] The University of Manchester: Aerodynamic Particle Sizer.

[23] The University of Manchester: Impactors and Filters.

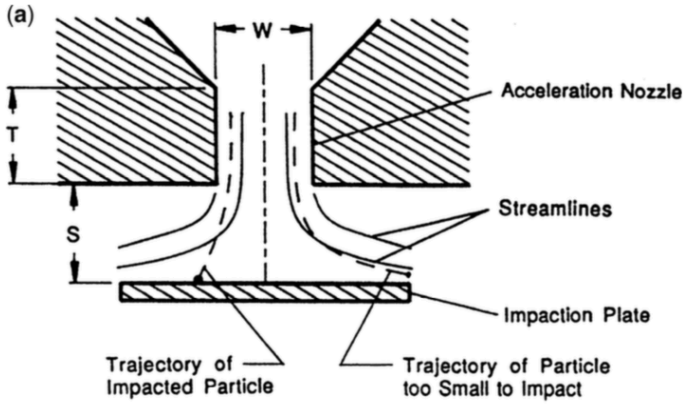

Figure 2.7: Schematic operation principle of single impactor[24]

Figure 2.7 presents the setup of a single impactor but more configurations are available. For instance, a cascade impactor is composed of several impactors in series with decreasing cutoff size. Cyclones are another variation of impactors; they combine the impaction with the gravitational settling of large particles which get stuck into the wall before arriving to the collecting plate. Another concept is the virtual impactor which uses a virtual space of slow flow instead of a plate to separate particles.

With impactors, mass distribution can be determined by weighting the plates before (initial mass) and after (final mass) performing a test. With the initial and final mass, net mass is also known, and then, mass fraction can be calculated.

2.2.5 Other methods

Apart from the instruments previously explained, other real-time techniques are available to analyze aerosol particles.

Differential Mobility Analyzers (DMA) separate aerosol particles according to their electrical mobility. It consists of a cylinder with a charged central rod. Sheath air, which is not affected by electrical mobility, is the main flow and aerosol flow is injected towards the inner wall of the cylinder. Particles will move to the central rod at a velocity which depends on their electrical mobility. A gap is located at a certain point of the rod, and only particles with a determined charge, and certain size, will pass through the gap.

Scanning and Differential Mobility Particle Sizer Spectrometers (SMPS/DMPS) consist of a DMA and a CPC to measure size distribution and concentration. The voltage is increased continuously (SMPS) or stepwise (DMPS) and electrical mobility distribution is measured. The number concentration for each mobility bin is measured by the CPC. Size distribution can also be calculated by using a computer inversion routine.

Other techniques such as Particle charging, based on charging particles with positive and negative gas ions, are also used to measure aerosol characteristics.

[24] Baron, P. A. et al.: Aerosol measurement (2011), p.135.

2.3 Aerosol losses

To transport aerosol from the sampling points to the measurement instruments some length of tube is required. Aerosol sample characteristics such as number concentration or size distribution would be the same at the sampling point and at the measuring point using an ideal sample transport system. However, sampling and transport systems are not ideal and, consequently, losses should be taken into consideration. In order to obtain a representative aerosol sample, the sampling and transport of particles must be optimized. In this section, a summary of sampling and transport mechanisms which cause particle losses is presented.

2.3.1 Sampling losses

The sampling efficiency can be described as the fraction of aerosol particles that enter the sampling probe and successfully reach the transport tubing.[25] First, if direction of the aerosol flow respect to the sampling tube is parallel or, in other words, there is no inclination between them, the sampling is isoaxial. In non-isoaxial cases, when the angle between flow and sampling tube is bigger than 0º, large particles losses are produced due to the impossibility to follow the flow streamlines.

Another important factor is the velocity ratio between the ambient gas velocity (U_o) and the sampling gas velocity (U).[26] When both velocities are equal, the sampling is isokinetic ($U_o = U$). If velocities are not equal, the sampling is non-isokinetic, being super-isokinetic when $U_o<U$, and having large particles losses, or sub-isokinetic when $U_o>U$, and having small particles losses. In all the cases, the sampling is assumed to be isoaxial. Therefore, achieving isokinetic sampling is a requirement to get the highest possible sampling efficiency.

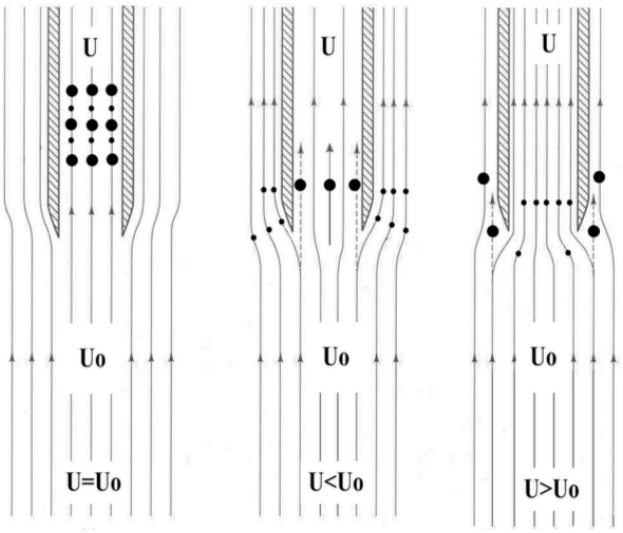

Figure 2.8: Streamlines in isoaxial sampling[27]

[25] Weiden, S.-L. von der et al.: Particle Loss Calculator (2009), p.481.

[26] Baron, P. A. et al.: Aerosol measurement (2011), p.75.

[27] Gregory D. Wight: Fundamentals of air sampling (1994).

2.3.2 Transport losses

During transport through sampling tubes, losses are produced due to some deposition mechanisms. In this section, the most common ones will be overviewed. These mechanisms are diffusional deposition, gravitational settling deposition or sedimentation, inertial deposition in bends and constrictions amongst others.

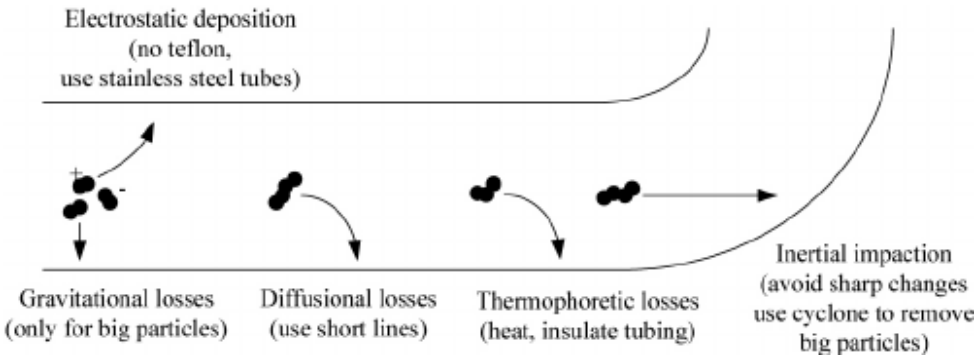

Figure 2.9: Summary of transport losses[28]

2.3.2.1 Diffusional deposition

Brownian motion refers to the random movement of particles due to their collision with molecules of the fluid. Small particles experimenting Brownian motion will disperse from areas with high to low concentrations. Therefore, particles will diffuse toward the surface of a tube and will be deposited there since it acts as a sink for the particles that are diffusing.[29]

2.3.2.2 Gravitational settling deposition or sedimentation

Gravitational forces affect particles through the transport lines. Particles settlement is produced due to their weight causing deposition on the lower inner surface of the tube. It has to be considered that in vertical tubes there is no horizontal surface on where particles can be deposited. Accordingly, gravitational losses in vertical tubes are 0%. For inclined tubes, efficiency is related with the angle of inclination.

2.3.2.3 Inertial deposition in bends and constrictions

In bends, the direction of flow is changed and, consequently, large particles cannot follow it because of their inertia. When flow is laminar, secondary recirculation flow patterns develop that push the axial flow core to the outside of the bend and that causes particle deposition.[30] The parameters that affects inertial deposition in bends are curvature ratio (R_0), Reynolds number and Stoke number.

[28] Giechaskiel, B. et al.: Sampling of Non-Volatile Vehicle Exhaust Particles (2012), p.8.

[29] Baron, P. A. et al.: Aerosol measurement (2011), p.90.

[30] Baron, P. A. et al.: Aerosol measurement (2011), p.100.

The effect of the curvature ratio (R_0), which is the radius of the bend divided by the radius of the tube, is negligible when $5 \leq R_0 \leq 30$.[31] Reynolds number is a dimensionless number and expresses the ratio of inertial forces to viscous forces. It is used to predict flow patterns in fluids. Stokes number is also a dimensionless number which gives the ratio of a particle response time to the characteristic time scale of the flow and is generally used as an indicator of similitude in particle behaviour in a given aerosol flow configuration.[32]

In constrictions, the direction of flow is also changed. Large particles which cannot follow the flow, as in bends, will deposit on the walls in front of the constriction.

2.3.2.4 Other deposition mechanisms

Apart from the previous ones, there are other factors that can influence on the transport of particles. For instance, turbulent inertial deposition is produced when, under turbulent regime flow, large particles are not able to follow the flow streamlines because of their inertia. As a consequence, these particles are deposited on the tube surface.

Losses due to electrostatic deposition are also present in the aerosol transport systems. Static charge in tubes can produce deposition in charged particles.[33] In order to avoid this kind of losses, conductive tubes must be used to prevent the creation of electrical fields that can induce particle deposition.

Another phenomenon is the so-called thermophoresis. It occurs when there is a gradient of temperature, then particles will move from high to low temperatures. Otherwise, when deposition is produced by a concentration gradient the phenomenon is called diffusiophoresis.

[31] Pui, D. Y. et al.: Particle Deposition in Bends (1987), p.303.

[32] Baron, P. A. et al.: Aerosol measurement (2011), pp. 24–39.

[33] Baron, P. A. et al.: Aerosol measurement (2011), p.95.

3 Concepts for measurements in test drives

In this chapter, the concepts developed during this Bachelor thesis to carry out brake particles measurements in real-drives are presented. The first concept consists of a full brake enclosure device while the second concept deals with a sealing of the rim with the objective of obtaining more realistic conditions. With these setups, measurements of number concentration and size distribution are expected to be achieved. In the next points, the basic operating principles of each concept are explained.

3.1 Analysis of requirements

The development of these concepts has to fulfill some requirements. First of all, it is essential to minimize losses of particle number by sealing the collecting shell from the exterior. With that, particles cannot enter or leave the enclosure, and only particles emitted by the brake would be read. Another requirement is the necessity of achieving particle size independent sampling efficiency so as to get representative samples of the particles emitted. Finally, realistic conditions in the collecting shell, regarding flow conditions and interaction of particles with vehicle components, have to be created to obtain realistic samples of particles.
In order to develop solutions for the requirements above mentioned, morphological boxes have been used. Critical problems are determined and then many possible solutions, with their advantages and disadvantages, are identified. With this system, illogical solution combinations can be eliminated.

3.2 Full brake enclosure device

The main purpose is to control the cleanness of the surrounding air of the brake and sample particles emitted directly by the brake. This concept, sucking out clean air and using isokinetic sampling was designed by IUTA (Institute of Energy and Environmental Technology e. V) and was mounted in a dynamometer test stand. The full enclosure device around the brake to collect particles and minimize losses was used by Daimler in a real car. However, the enclosure device was not totally sealed, and had some spots where particles could enter and leave.

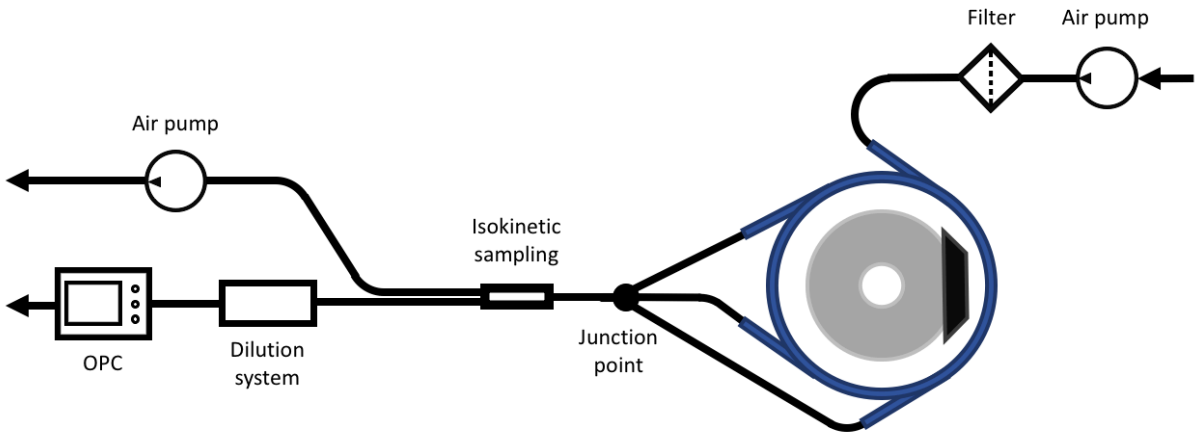

Figure 3.1: Schematic operation principle of the full brake enclosure device system

Airflow from the front part of the car is sucked by a pump and cleaned by an HEPA filter. The clean air enters in the brake enclosure device which is completely sealed from the exterior, preventing particles entering or leaving the enclosure. Several outlets are placed around the collecting box to take samples of brake particles.

The pump helps to increase the air flow through the tubes. When using a pump, the volume flow inside the collecting shell is determined by the power of the pump and, in this way, the concentration can be calculated. Finally, a dilution system before the OPC sensor reduces the concentration of particles.

To develop the collecting box some points have to be considered. First, the space is very limited and the movement of some parts of the vehicle in the inner part of the brake such as the steering rods hinder the design of the enclosure device. These facts make necessary a complex geometry of the box which has to be taken into consideration to select the appropriate method of construction.

Then, to seal the enclosure device, the use of different types of sealing are necessary. Rotary sealing has to be used for the outer part of the collecting box since there are no static points to seal the box with the brake. For this reason, some particles can be emitted because of the friction between the sealing material and the part in contact with it. This could lead to contamination of particle samples. Another fact is the high temperature reached by the brake. That has to be considered to select the suitable sealing and shell materials.

This approach of sealing the entire brake to minimize losses gives the opportunity to get trusty results, only particles emitted by the brake would be sampled, but not a realistic behavior since the flow conditions are conditioned by the enclosure device and the applied flow stream by the pump. If an ideal sealing was achieved, the results should be the same or similar as those obtained in the IUTA dynamometer and, therefore no additional information would be gained.

A concept of a full enclosure devices could look similar to the one shown in the Figure 3.2.

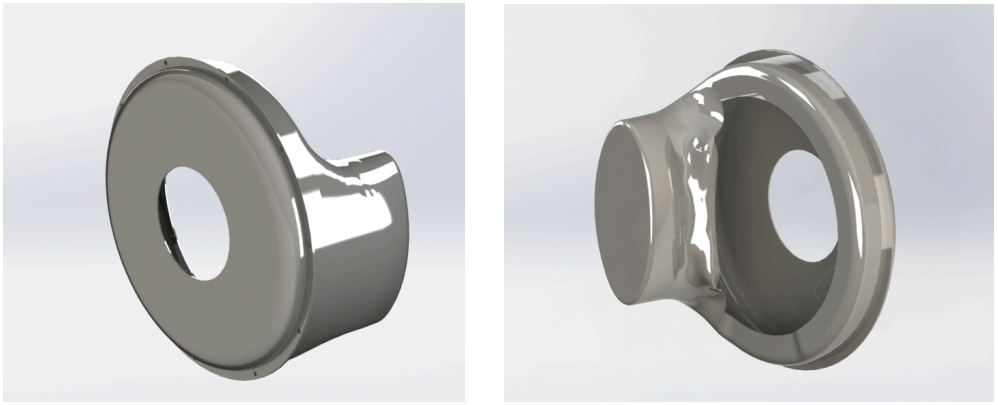

Figure 3.2: Full brake enclosure device concept

3.3 Rim shell device

This concept has been developed in order to get more realistic conditions around the brake. The cleanness is also controlled but the interaction of the flow with the rim try to simulate the conditions of a real car.

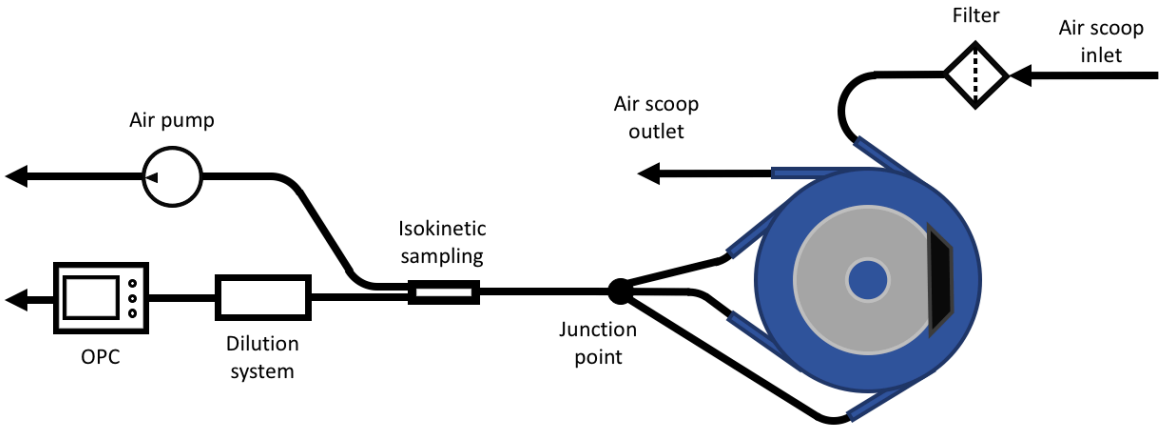

Figure 3.3: Schematic operation principle of the rim shell device concept

Apart from the inner part of the rim, the spots are also sealed. Air enters to the room through an air scoop and an HEPA filter cleans it. This duct is located in the lower part of the flat shell pointing directly to the bottom part of the front of the car. A study carried out by Körner et. al.[34] in a wind tunnel with a transparent front wheel has shown that under the bumper, the flow is higher than in other parts around the wheel. The flow entering inside depends on the velocity of the air flow and the dimensions of the air scoop. A flow velocity measurement device is installed in parallel to the duct. By measuring flow velocity and knowing the area of the scoop, the air flow entering to the room can be determined. Part of the flow leaves the room through an air scoop outlet with an HEPA filter. This filter is used to prevent other particles entering inside the room. The functioning principle is shown in the Figure 3.4

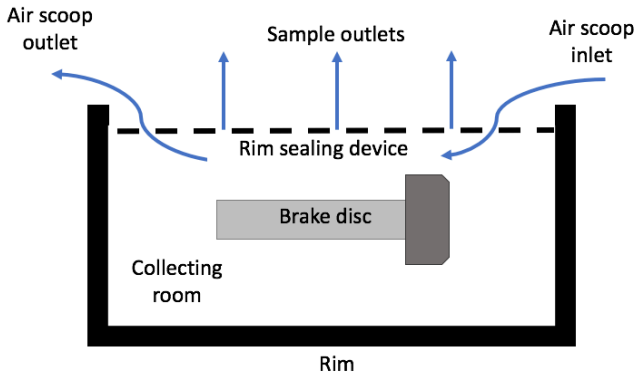

Figure 3.4: Rim shell device functioning

[34] Körner, M. et al.: Untersuchung der Bremsscheibenumströmung an einem Windkanalmodell (2007).

Augsburg et al.[35] performed simulations with CFD software and Particle Image Velocimetry (PIV) to analyze the trajectory of particles in the rim and found that particles tend to recirculate around the brake and propagate to the upper part of the rim. The Figure 3.3 shows the results obtained in the study. From the study carried out by Augsburg et al. can be deduced that the air scoop outlet can be located in the upper part of the rim since the flow tends to go in that direction.

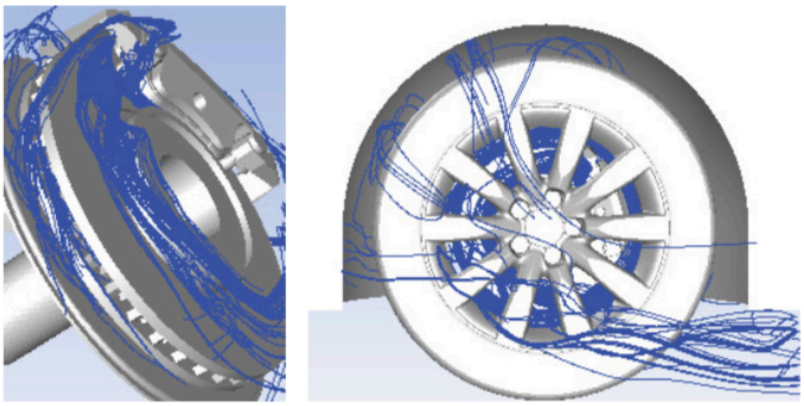

Figure 3.5: Trajectory of particles through the rim

Parallel to the outlet and within the exit area of the air scoop, another flow velocity measurement device is installed to determine the air flow escaping from the rim. As in the air scoop inlet, by measuring the velocity and knowing the dimensions of the air scoop, the flow leaving the collecting shell can be calculated. Knowing the air flow entering and leaving the rim, the air flow which remains inside the room can be calculated.

For the sealing of the rim, the heat shield could be substituted for a flat metal sheet which covers all the rim circular section. A material which can withstand rotary speed, such a brush, should be used to seal the gap between the flat metal sheet and the rim. For the flow measurement device, a pitot tube could be used since it is very precise. To calculate the flow velocity the measuring principle of the pitot tube is based on the pressures difference.

Some particles would stick on the rim surface and airborne particles would be pulled out of the rim by a pump, as in the concept shown in the previous section, through several outlets distributed around the shell. This permits an approach to a more realistic behavior of the particles inside the rim since flow conditions are not conditioned by the enclosure device. That implies that the flow inside the rim is not laminar and, consequently, the particles taken from the collecting shell would not ensure a representative sample. Due to this fact and the limited time available, the construction of the rim shell device has not been possible.

[35] Augsburg, K. et al.: Characterization of particulate emissions (2011), p.7.

3.4 Conclusions

To finish this chapter, conclusions extracted from the development of both concepts are presented in this section.

With the full brake enclosure device, the cleanness of the surrounding air of the brake system is controlled. That means that particles cannot leave the collecting shell, and particles from the exterior cannot enter inside. The use of a pump to pull clean air inside the enclosure device and the non-interaction of the flow with the rim surfaces prevent the achievement of realistic flow conditions. After considering this setup, it was discarded because if an ideal sealing of the enclosure device is assumed, no information would be gained respect to the tests performed in the IUTA dynamometer where the same concept has been used.

Regarding the rim shell device, the cleanness is also controlled. In addition, a more realistic approach can be achieved due to the flow conditions inside the rim and the interaction of the flow with the rim surfaces. However, the non-laminar flow inside the rim makes difficult to take representative particle samples. This fact and the little time available to manufacture the rim shell device and assembly the setup have been decisive to reject its construction. However, the development of this concept could be considered for future works.

4 Study of aerosol transport efficiency

In this chapter, some of the losses overviewed in the section 2.3.2 will be studied. A theoretical calculation of the efficiency will be done. The mechanisms of losses which will be object of study have been chosen considering the background of this Bachelor thesis. Only the ones that can be optimized will be taken into consideration. For this reason, diffusional deposition, gravitational settling deposition in horizontal and inclined tubes and inertial deposition in bends will be studied. In addition, efficiency of a particle transport system similar to one that could be used in a test car will be calculated.

Some parameters have been assumed to perform the study. Before anything else, the fluid properties have been selected regarding the instruments available in the FZD department. Accordingly, dry air (at 20ºC) is assumed to be the fluid because it is the fluid taken in the inlet of the aerosol generator, and DEHS ($C_{26}H_{50}O_4$) is the liquid contained in the aerosol generator, AGF 2.0 from Palas, to produce aerosol droplets. These parameters have chosen in order to perform experimental tests in future works with the instruments available in the FZD department and compare the experimental results with the theoretical ones obtained in this Bachelor thesis.

DEHS (C26H50O4)	
Molecular weight	426,68 g/mol
Density (ρ)	912 kg/m^3
Dynamic viscosity (μ)	0,022 Pa·s

Table 4.1: DEHS properties[36]

DRY AIR	
Temperature (T)	20 ºC
Air viscosity (η)	0,0000182 Pa·s
Air density (ρ)	1,2048 kg/m^3
Mean free path (λ)	0,0665 μm

Table 4.2: Air properties[37]

[36] Palas GmbH: DEHS properties.

[37] McQuillan, F. J. et al.: Properties of dry air (1984).

The tubes used for the transport of particles are conductive, eliminating electrostatic deposition losses, and have a diameter of 6 mm which is the characteristic parameter of the tubes to calculate Reynolds number. Flow regime is assumed to be laminar, that occurs when $Re < 2000$[38], in order to minimize losses in the system. With laminar flow, turbulent inertial deposition losses are not expected to occur in the transport system. Other losses like thermophoresis and diffusiophoresis will not be studied. Having a fixed diameter, 6 mm, flow regime depends on the flow rate (Q) which can be adjusted in the aerosol generator. Therefore, to achieve laminar flow regime:

$$Re = \frac{\rho \cdot U \cdot d}{\mu} \tag{4.1}$$

by substituting in the Equation 4.1 the parameters of air density (ρ) and air viscosity (μ) from Table 4.2, the diameter of the tube ($d = 6\,mm$) and the maximum Reynolds number for laminar flow ($Re = 2000$), the velocity of the fluid in the tube (U) can be calculated: $U = 5{,}0354\,m/s$. Now, flow rate (Q) can be determined applying:

$$Q = A \cdot U \tag{4.2}$$

where $A =$ area of the circular section of the tube. Then, $Q = 8{,}5424\,l/min$, which is the maximum flow rate to achieve laminar flow. $Q = 8{,}5\,l/min$ is taken to make easier the development of the study. Therefore, with the new Q, the new Reynolds number and fluid velocity is calculated: $Re = 1990$ and $U = 5{,}01\,m/s$. Several tube lengths will be studied, starting from 0,25 m up to 4 m. It has no sense to study longer lengths since they never will be set in the car. For the gravitational deposition in inclined tube and inertial deposition in bends, five angles between 0 and 90º and between 0 and 180º will be studied, respectively.

Parameters	
Diameter (d)	6 mm
Flow rate (Q)	8,5 l/min
Flow velocity (U)	5,01 m/s
Reynolds number (Re)	1990
Tube length (L)	0,25 – 4 m
Angles of inclination (θ)	0 – 90º
Angles of the bends (φ)	0 – 180º

Table 4.3: Summary of parameters used in the study

[38] Baron, P. A. et al.: Aerosol measurement (2011), p.17.

4.1 Particles size range

Some researchers such as Sanders et al.[39], in number distribution, or Kukutschkova et al.[40], in mass distribution, have reported that most of the particles lie in the range under 10 μm. It is essential to mention that in different type of tests conducted by Söderber et al.[41] the peak of number and volume distribution was about 0,3 and 3 μm, respectively. Wahlström et al.[42], using a brake test stand, also reported that the majority of particles have a diameter smaller than 1 μm.

Particle diameters which will be studied will be focused on the size range from 0,38 to 12 μm. Being the former size the lowest particle diameter that AlphaSense OPC N2 can read, which is the sensor available in the FZD department, and the latter size being two microns above 10 μm because, generally, the larger particles do not exceed that size. The steps between sizes are also the ones that the sensor can read. Furthermore, some sizes lower than 0,38 μm and up to 10 nm will also be included.

4.2 Theoretical losses

In this section, diffusional deposition losses, gravitational settling deposition losses in horizontal and inclined tubes and inertial deposition losses in bends will be calculated. Efficiency, which is the percentage of particles that will not be lost through the transport system, will be calculated for a range of particle diameters and tube lengths. It is to say that the total transport efficiency results from the product of efficiencies for each loss mechanism.

In the following sections the methodology followed to calculate efficiency will be shown for each mechanism. Note that all the formulas have been extracted from the book 'Aerosol measurement: Principles, Techniques, and Applications' written by Baron et al.[43] and are only valid for laminar flow regime ($Re < 2000$).

4.2.1 Diffusional deposition efficiency

As it has been explained in the section 2.3.2.1 these losses are directly related with Brownian motion and affect small particles. Diffusion efficiency is expressed as:

$$\eta_{diff} = e^{\left[-\frac{\pi \cdot d \cdot L \cdot V_{diff}}{Q}\right]} = e^{[-\xi \cdot Sh]} \tag{4.3}$$

[39] Sanders, P. G. et al.: Airborne Brake Wear Debris (2003), p.4068.

[40] Kukutschová, J. et al.: Wear performance and wear debris (2010), p.86.

[41] Söderberg, A. et al.: A Pin on Disc Simulation (2008), p.23.

[42] Wahlström, J. et al.: A disc brake test stand (2009), p.251.

[43] Baron, P. A. et al.: Aerosol measurement (2011).

where $Sh =$ Sherwood number and $V_{diff} =$ deposition particle velocity. The Sherwood number, which is a dimensionless mass transfer coefficient that relates the particle diffusive deposition velocity to the particle diffusion coefficient, for laminar flow can be calculated as:

$$Sh = 3{,}66 + \frac{0{,}2672}{\xi + 0{,}10079 \cdot \xi^{1/3}} \tag{4.4}$$

$$\xi = \frac{\pi \cdot D \cdot L}{Q} \tag{4.5}$$

being $D =$ particle diffusion coefficient, $L =$ tube length and $Q =$ flow rate in the tube. Particle diffusion coefficient is expressed as:

$$D = \frac{k \cdot T \cdot C_C}{3 \cdot \pi \cdot \eta \cdot d_p} \tag{4.6}$$

where $k =$ Boltzmann constant $= 1{,}38 \cdot 10^{-23}\ N \cdot m/K$, $T =$ absolute temperature, $C_C =$ Cunningham slip correction factor, $\eta =$ air viscosity and $d_p =$ particle diameter. Cunningham slip correction factor is used to correct Stokes law which is based on no-slip condition. It comes into account for small particles:

$$C_C = 1 + \frac{\lambda}{d_p}\left[2{,}33 + 0{,}966 \cdot e^{\left(-0{,}499\frac{d_p}{\lambda}\right)}\right] \tag{4.7}$$

where $\lambda =$ mean free path. Note that diffusive losses for laminar flow not depend on tube diameter.

4.2.2 Gravitational settling deposition efficiency

4.2.2.1 Horizontal tubes

In horizontal tubes, the equation for laminar flow which gives the efficiency is:

$$\eta_{grav,horizontal} = 1 - \frac{2}{\pi}\left[2 \cdot \varepsilon \cdot \sqrt{1 - \varepsilon^{2/3}} - \varepsilon^{1/3} \cdot \sqrt{1 - \varepsilon^{2/3}} + \arcsin\left(\varepsilon^{1/3}\right)\right] \tag{4.8}$$

$$\kappa = \varepsilon \cdot \cos(\theta) = \frac{3}{4} \cdot \frac{L}{d} \cdot \frac{V_{ts}}{U} \cdot \cos(\theta) \tag{4.13}$$

$$\varepsilon = \frac{3}{4} \cdot Z = \frac{3}{4} \cdot \frac{L}{d} \cdot \frac{V_{ts}}{U} \tag{4.9}$$

being Z = gravitational deposition parameter, L = tube length, d = tube diameter, U = flow velocity in the tube and V_{ts} = terminal settling velocity of the particles which can be expressed as:

$$V_{ts} = \frac{\rho_p \cdot g \cdot d^2}{18 \cdot \mu} \cdot C_C \tag{4.10}$$

where ρ_p = density of the particle and g = gravitational acceleration.

4.2.2.2 Inclined tubes

If the tube is inclined, the component of terminal settling velocity will be affected by the angle of inclination (θ) as $V_{ts} \cdot \cos(\theta)$, and then:

$$\eta_{grav,inclined} = 1 - \frac{2}{\pi}\left[2 \cdot \kappa \cdot \sqrt{1-\kappa^{2/3}} - \kappa^{1/3} \cdot \sqrt{1-\kappa^{2/3}} + \arcsin\left(\kappa^{1/3}\right)\right] \tag{4.11}$$

$$\kappa = \varepsilon \cdot \cos(\theta) = \frac{3}{4} \cdot \frac{L}{d} \cdot \frac{V_{ts}}{U} \cdot \cos(\theta) \tag{4.12}$$

It is only valid if:

$$\frac{V_{ts} \cdot \sin(\theta)}{U} \ll 1 \tag{4.14}$$

where the axial component of the terminal velocity of the particle has to be very small respect to flow velocity in the tube. If the angle of inclination is zero (θ = 0º) or, in other words, the tube is horizontal the Equation 4.11 is reduced to the Equation 4.8. The angles which will be studied have to be in the range between 0º and 90º.

4.2.3 Inertial deposition efficiency in bends

First of all, the curvature ratio will be assumed to stay between 5 and 30. As it was explained in the section 2.3.2.3, if the curvature ratio value remains in that range, its effect is insignificant. The formula to calculate efficiency in bends depends on the angle of the bend and on the Stokes number, and is expressed as:

$$\eta_{bends} = \left[1 + \left[\frac{Stk}{0{,}171}\right]^{0{,}452 \cdot \frac{Stk}{0{,}171} + 2{,}242}\right]^{-\frac{2}{\pi} \cdot \varphi} \tag{4.15}$$

where $\varphi =$ angle of the bend is in radians. The Stokes number is a dimensionless number which characterizes the behaviour of particles suspended in a fluid. It expresses the ratio of a particle response time to the characteristic time scale of the flow, and can be determined as:

$$Stk = \frac{\tau \cdot U}{d} \tag{4.16}$$

where $U =$ fluid velocity in the tube, $d =$ characteristic parameter of the tube (diameter) and $\tau =$ particle relaxation time which is defined as:

$$\tau = \frac{\rho_p \cdot d_p^2}{18 \cdot \eta_f} \cdot C_C \tag{4.17}$$

being $\rho_p =$ density of the particle, $d_p =$ particle diameter and $\eta_f =$ fluid viscosity. The angles which will be studied have to be in the range between 0º and 180º.

4.2.4 Vehicle test transport system efficiency

In order to get an approach of the magnitude of losses in a real vehicle test, a sketch of the sampling lines has been designed based on the transport system used in previous FZD tests. The transport system goes from the measurement point, located in the cockpit of the car, to the collecting box of particles, near the calliper.

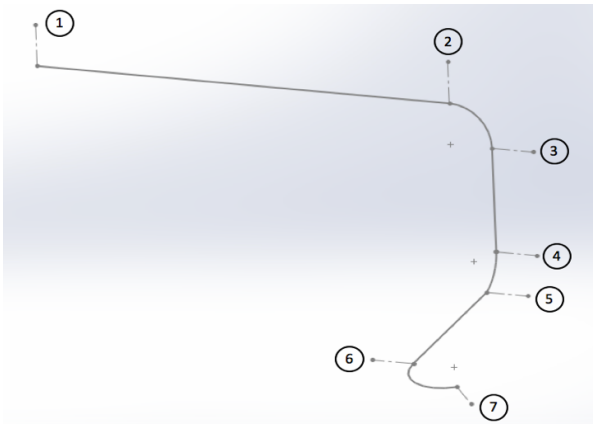

Figure 4.1: Sketch of the particles transport system

The measurement point is located in point 1, while the sampling point is in point 7. With the purpose of calculating the total losses of the system, it has been divided in 6 sections. The characteristics of each section are shown in the Table 4.8. All the bends have been assumed to have a radius of 100 mm, therefore the curvature ratio remains between 5 and 30.

Section	Points	Tube length	Other characteristics	Types of losses
1	1-2	1 m	Horizontal tube	Diffusional + Gravitational
2	2-3	0,16 m	Angle of the bend = 90º	Diffusional + Inertial in bends
3	3-4	0,25 m	Vertical tube	Diffusional
4	4-5	0,10 m	Angle of the bend = 120º	Diffusional + Inertial in bends
5	5-6	0,35 m	Angle of inclination = 15º	Diffusional + Gravitational
6	6-7	0,21 m	Angle of the bend = 60º	Diffusional + Inertial in bends

Table 4.4: Characteristics of the transport system

To calculate the total efficiency of the transport system the following expression is used:

$$\eta_{transport} = \prod_{tube\ sections} \left(\prod_{mechanisms} \eta_{tube\ section,mechanism} \right) \tag{4.18}$$

The total efficiency of the transport system results from the product of the transport efficiencies for all sections and for all mechanisms of losses. Losses for each mechanism are calculated as in the previous sections.

4.3 Results

In this section, the theoretical results for the chosen particle diameter size range will be analyzed. To do that, several graphics show the relation between efficiency and particle diameter for different tube lengths or angles and for each mechanism of losses. Graphics have been divided in fine ($d_p < 1$ μm) and coarse particles ($d_p > 1$ μm). Other size ranges to classify particles according its size can also be found in the literature.

The following figure shows the average of losses of all tube lengths or angles, for fine and coarse particles, for each mechanism. As it can be seen, the percentage of losses is higher for large particles because of their weight and inertia, except for diffusional deposition mechanism which depends on Brownian motion, and it affects small particles as it has been explained in chapter 2. The highest percentage of losses, around 20%, is related with inertial deposition in bends.

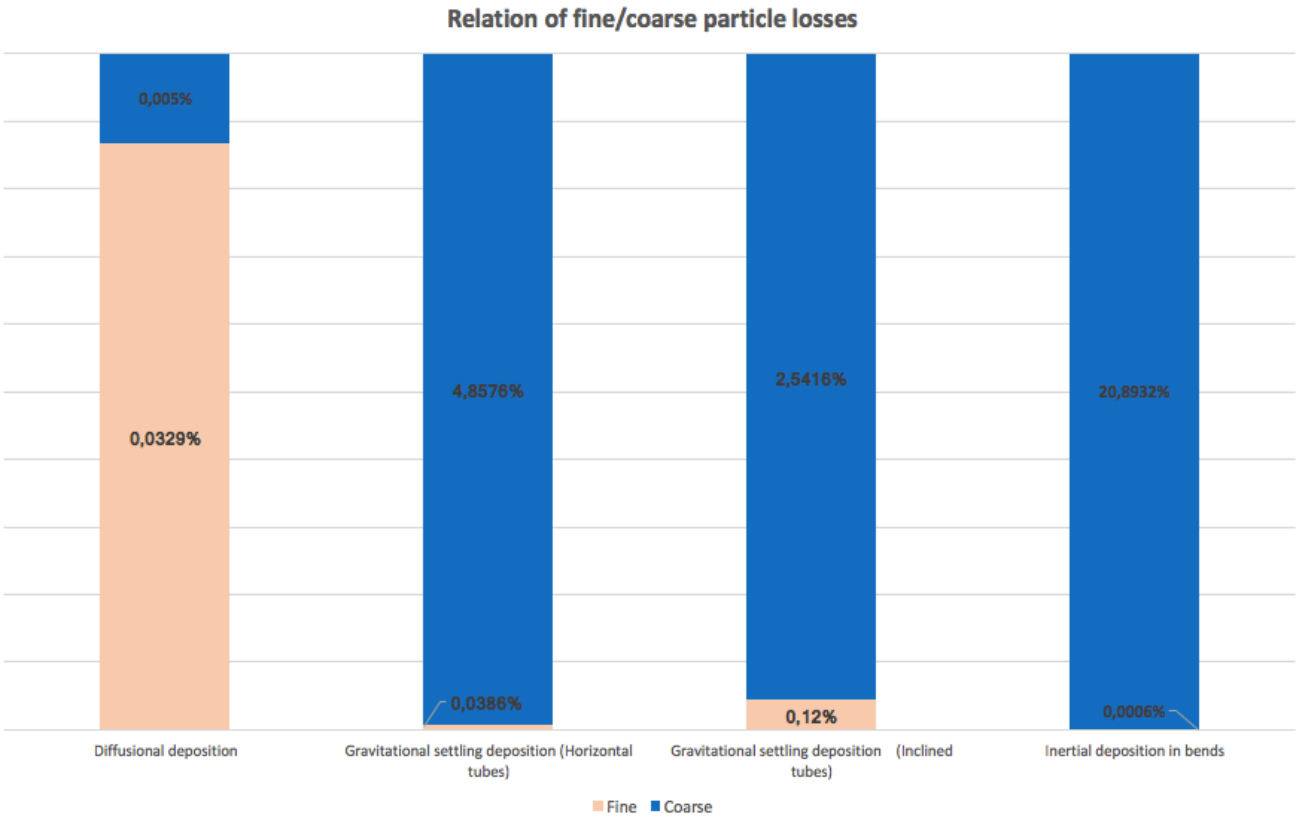

Figure 4.2: Graphic of fine/coarse particles losses relation

4.3.1 Diffusional deposition efficiency

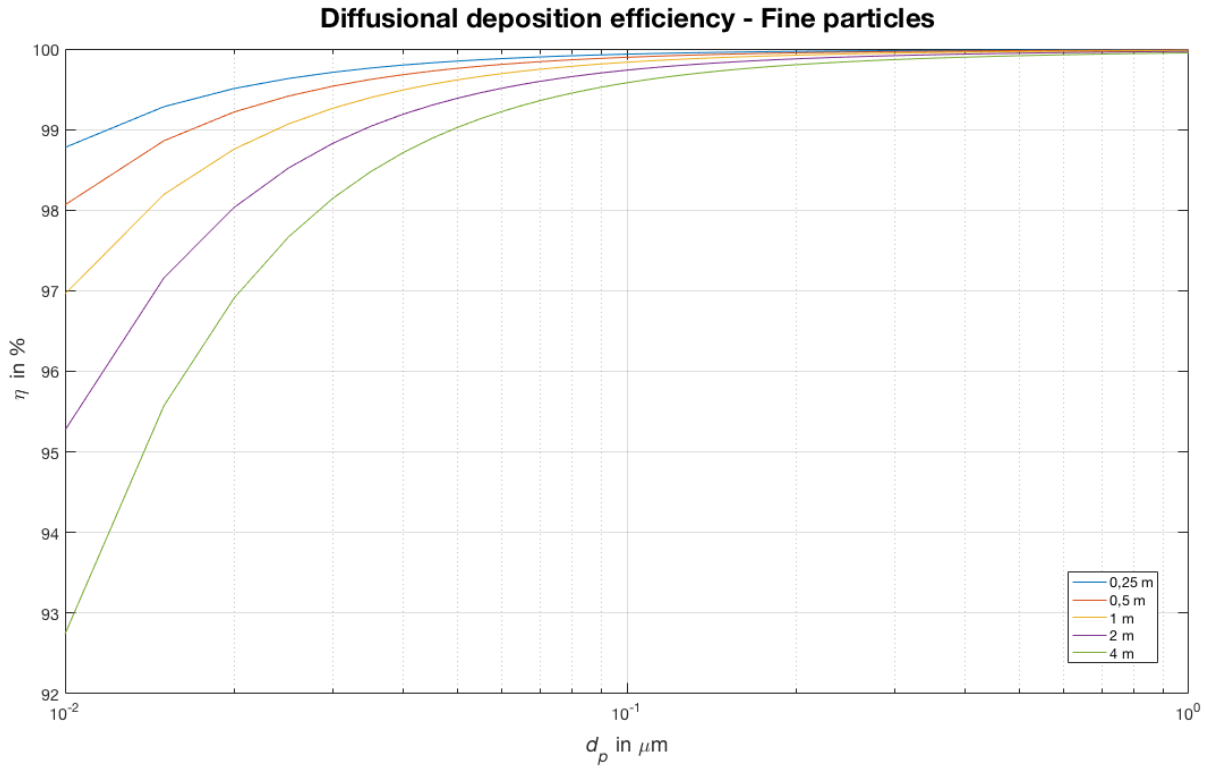

Figure 4.3: Graphic of diffusional deposition efficiency (Fine particles)

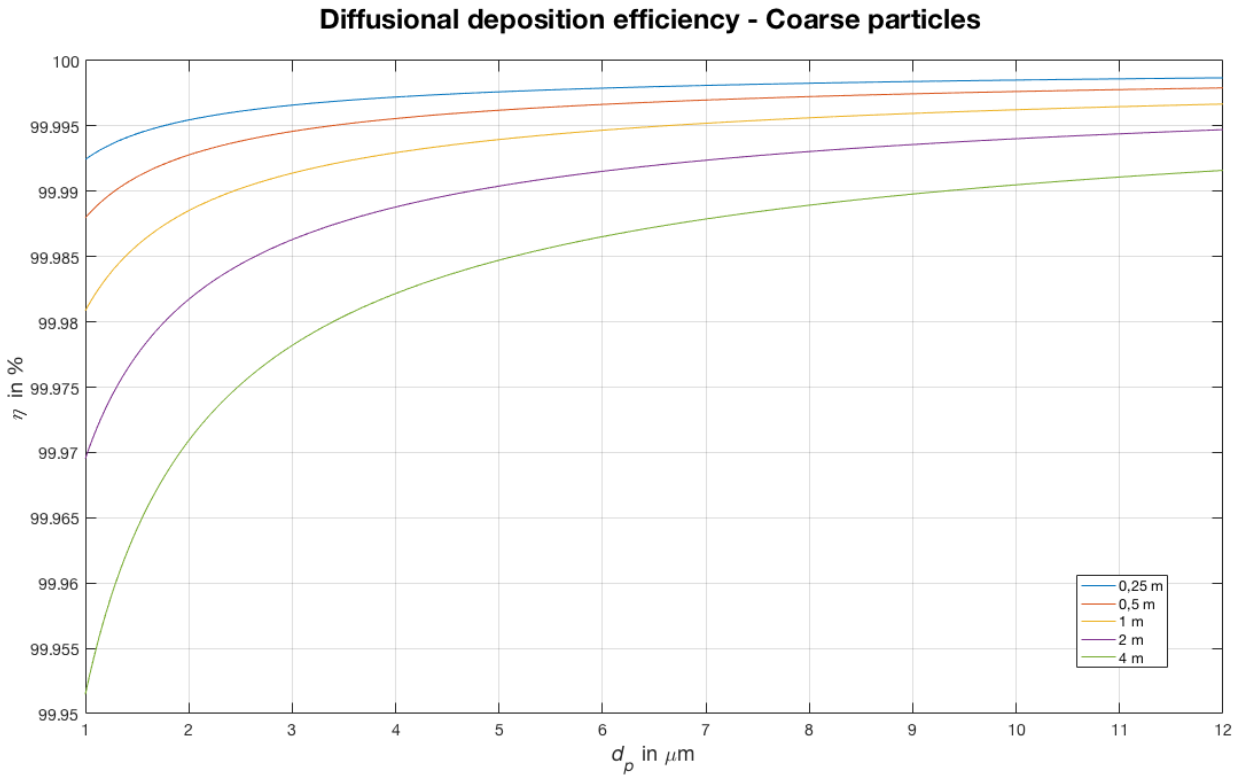

Figure 4.4: Graphic of diffusional deposition efficiency (Coarse particles)

As it is shown in the Figure 5.2, diffusional deposition affects small particles. For particles larger than 100 nm, losses are less than 1% and tend to approach to 100% efficiency when particle size increases. For particles smaller than 100 nm, efficiency decreases dropping below 99% and 93% for particles of 10 nm of diameter in a tube length of 0,25 m and 4 m, respectively.

For coarse particles, efficiency is very high. Losses for the worst case of the study, 4 m of tube length, are less than 0,05%. After observing Figures 5.2 and 5.3, it can be concluded that diffusional deposition depends on the length of the tube. Therefore, by reducing tube length, losses are cut down.

4.3.2 Gravitational settling deposition efficiency

4.3.2.1 Horizontal tubes

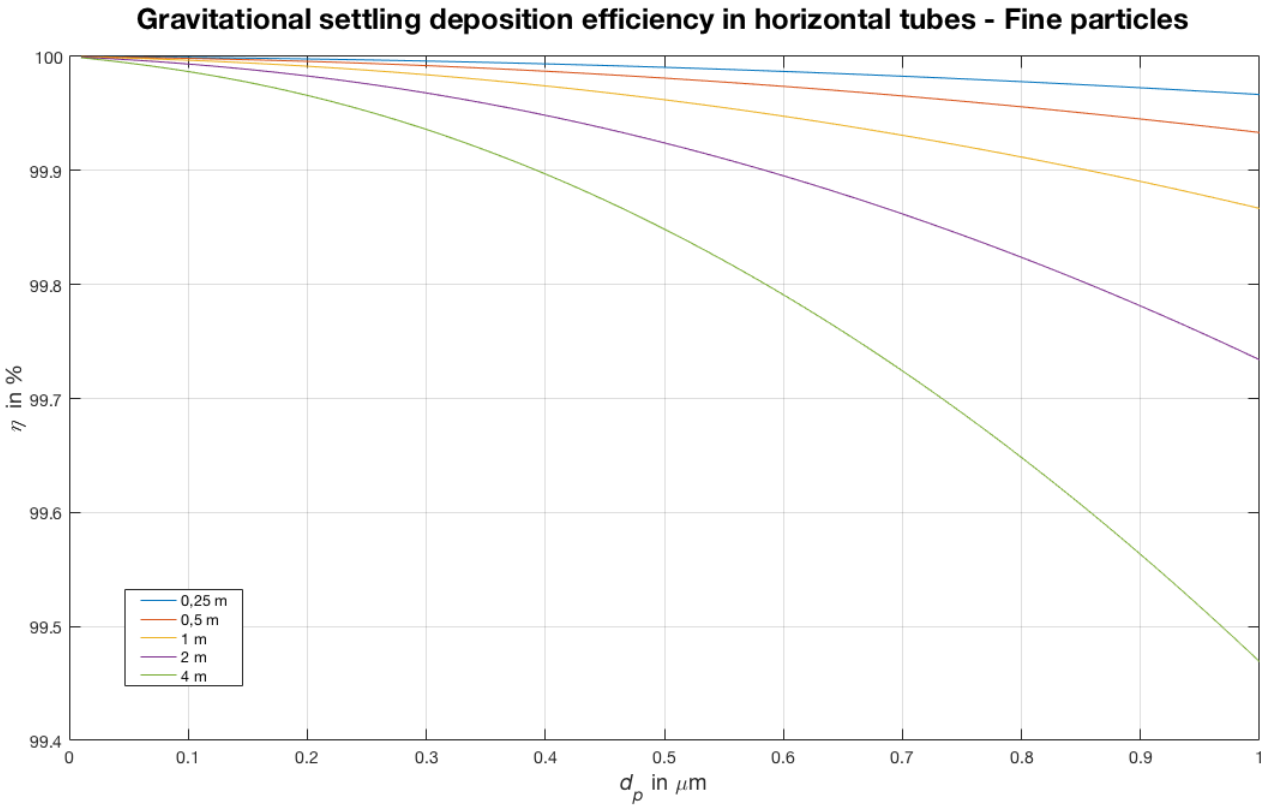

Figure 4.5: Graphic of gravitational settling deposition efficiency in horizontal tubes (Fine particles)

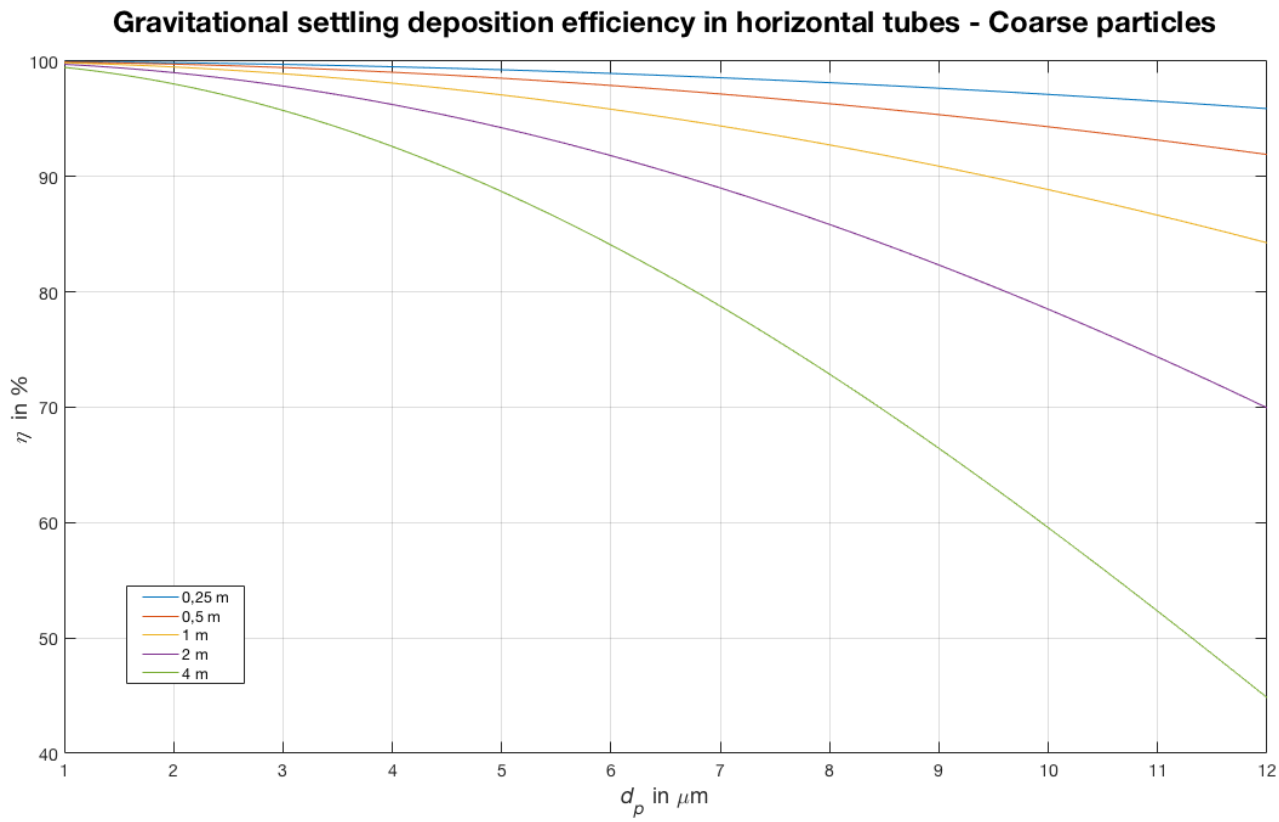

Figure 4.6: Graphic of gravitational settling deposition efficiency in horizontal tubes (Coarse particles)

For particles down micron size, efficiency tend to approach to 100% being over 99,9% for particles up to about 0,4 μm for all the tube lengths studied. When particles size reach 1 μm, efficiency decreases considerably. Although for tube lengths of 0,25 and 0,5 m efficiency remains over 99,9%, for tube lengths of 4 m it goes down until 99,5%.

For particles larger than a micrometer, efficiency remains over 90% up to sizes slightly above 4 μm. Efficiency decreases substantially as particle diameter grows. For particles with 12 μm of diameter, largest particle size studied, efficiency goes down 70 and 50% for tube lengths of 2 and 4 m, respectively. On the other hand, for tube lengths shorter than 0,5 m, losses are less than 10%. Gravitational settling deposition losses depend on the weight and inertia of the particles. As can be seen, this mechanism of losses also depends on the tube length.

4.3.2.2 Inclined tubes

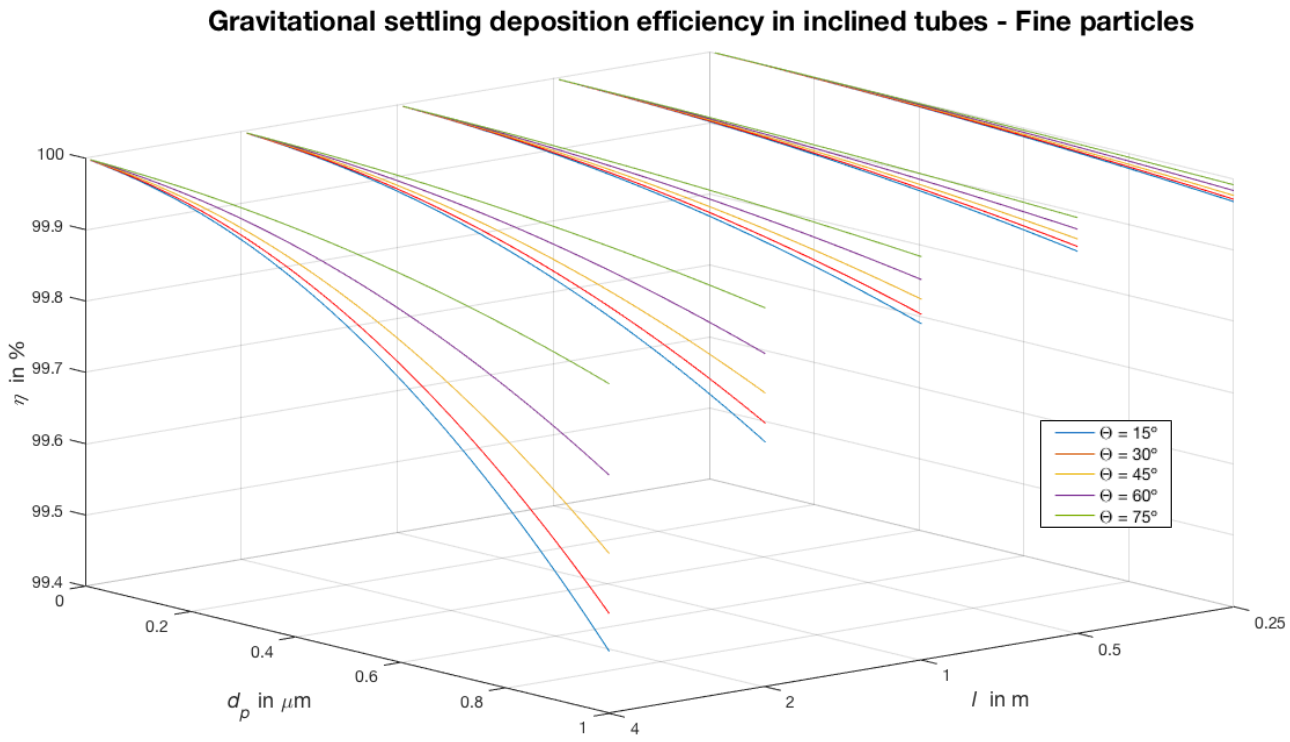

Figure 4.7: Graphic of gravitational settling deposition efficiency in inclined tubes (Fine particles)

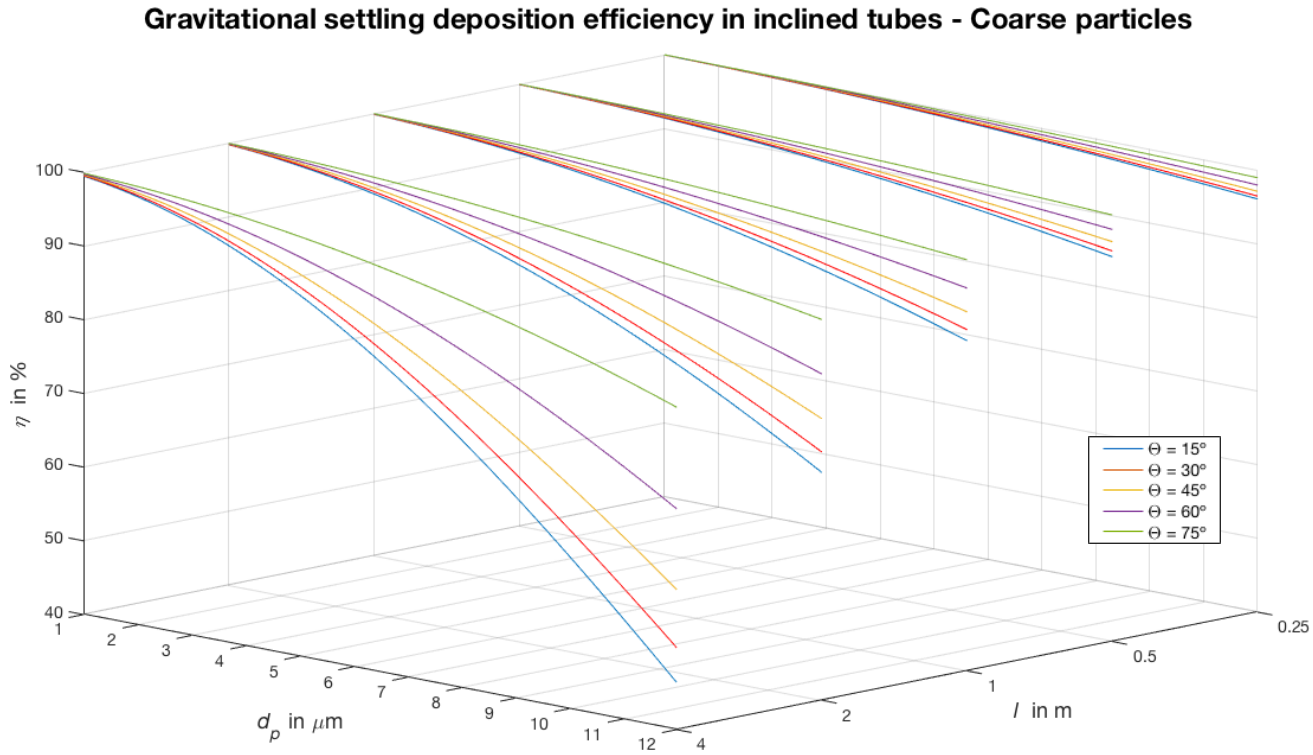

Figure 4.8: Graphic of gravitational settling deposition efficiency in inclined tubes (Coarse particles)

For fine particles, efficiency remains over 99,4% for all the tube lengths studied. Up to 0,5 m length losses are less than 0,1% for all angles of inclination. When the pipe tends to be vertical efficiency increases considerably. This is because the horizontal area where particles can deposit by gravitation decreases when angle of inclination raises.

For coarse particles, losses are less than 10% for all tube lengths up to a particle diameter about 5 μm. Efficiency remains over 50% for all the particle diameters and tube lengths except for particles of 12 μm and 4 m of tube length.

As can be seen in Figures 5.7 and 5.8, the difference of efficiency between angles is higher for large angles (over 45º) than for small angles or when the pipe tends to be horizontal.

4.3.3 Inertial deposition efficiency in bends

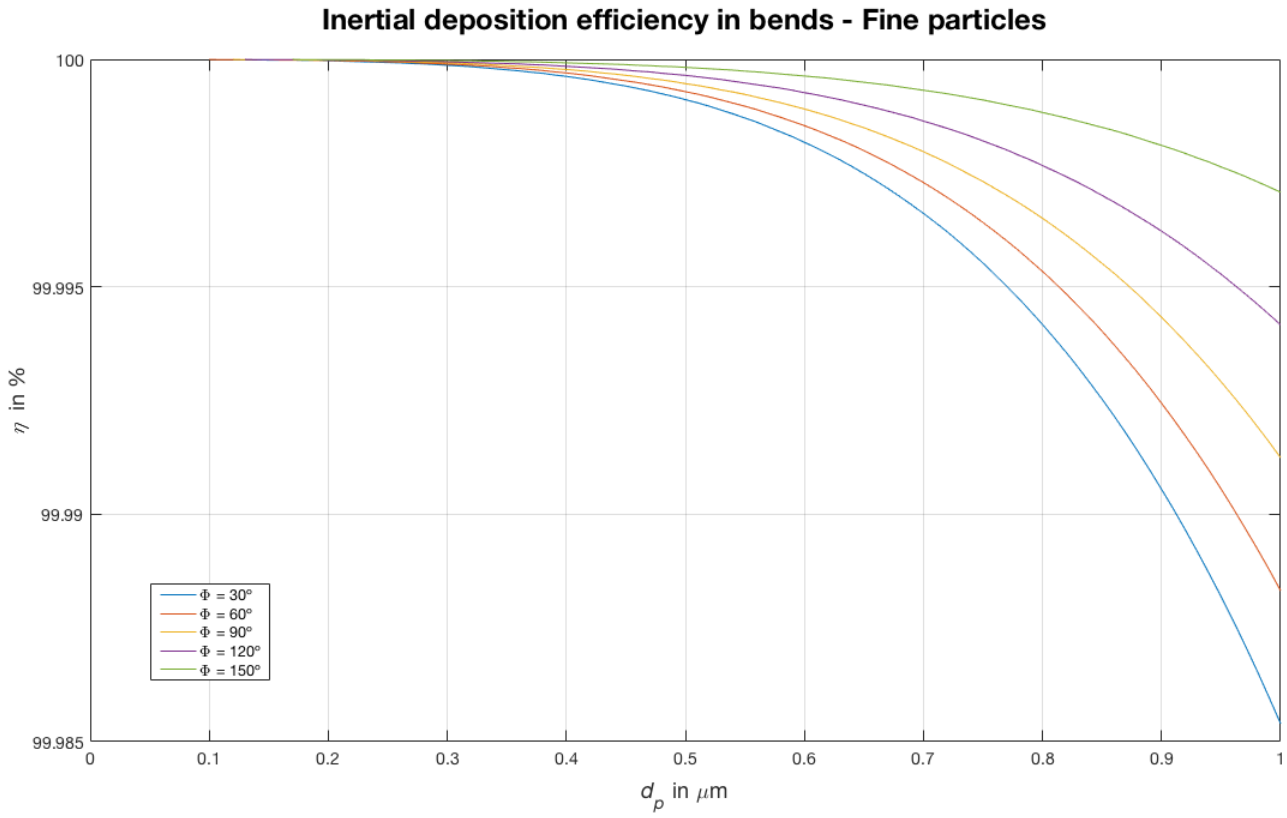

Figure 4.9: Graphic of inertial deposition efficiency in bends (Fine particles)

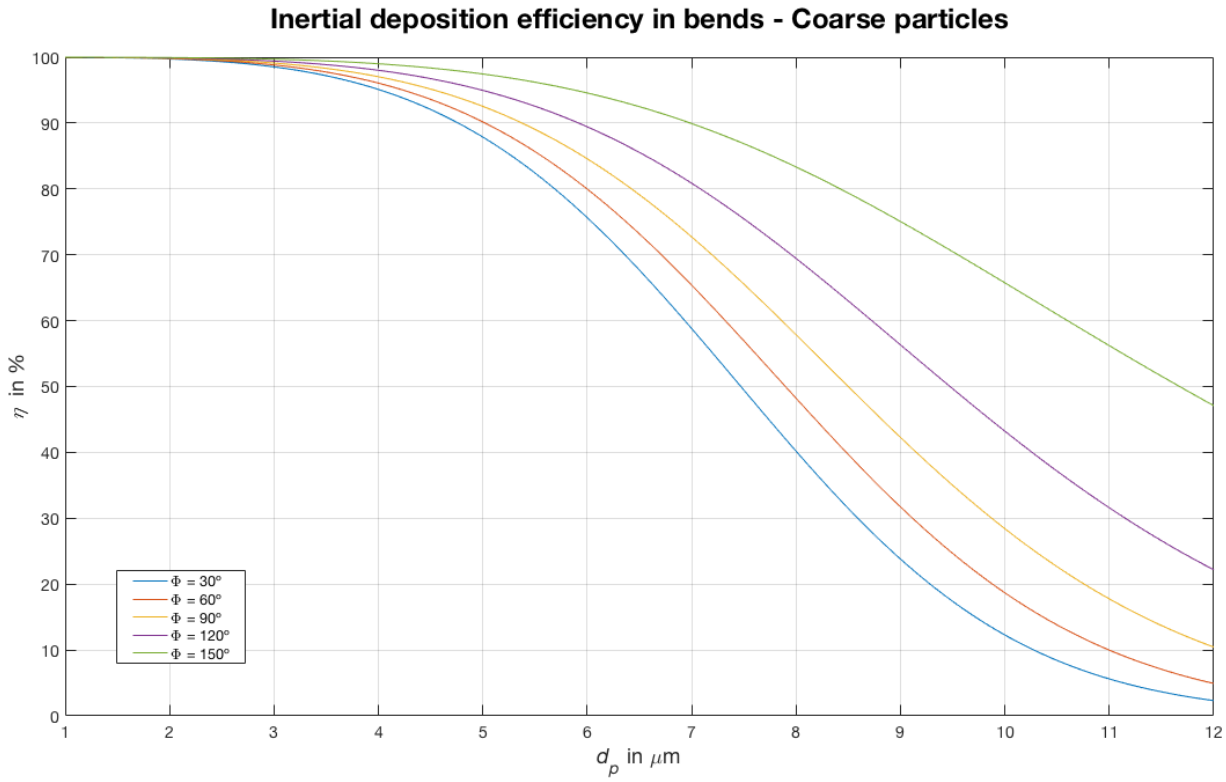

Figure 4.10: Graphic of inertial deposition efficiency in bends (Coarse particles)

Fine particles, as it is shown in the Figure 5.9, are almost not affected by inertial deposition in bends. For all the particles smaller than a micrometer, efficiency does not go down 99,985% for the worst cases studied. Due to their low weight and inertia, fine particles are able to follow the flow streamlines through bends.

For coarse particles, up to about 3 μm, efficiency remains close to 100%. For larger particles, losses increase heavily. Up to particles of 7,5 μm diameter, efficiency stills being higher than 50% for all angles studied. But when particles exceed 10 μm, losses are higher than 50% except for angles over 150º. For the largest particles of the study, 12 μm of diameter, efficiency is less than 5% for angles under 60º, which means that almost none particles can be read. There is a difference of 45% efficiency between using an angle of 30º or 150º.

Inertia of particles has a key role through the bends, and big particles cannot follow the flow and deposit to the walls. To reduce this kind of losses, small angles of bends have to be used since it has been seen that efficiency decreases substantially when angles become smaller.

4.3.4 Test vehicle transport system efficiency

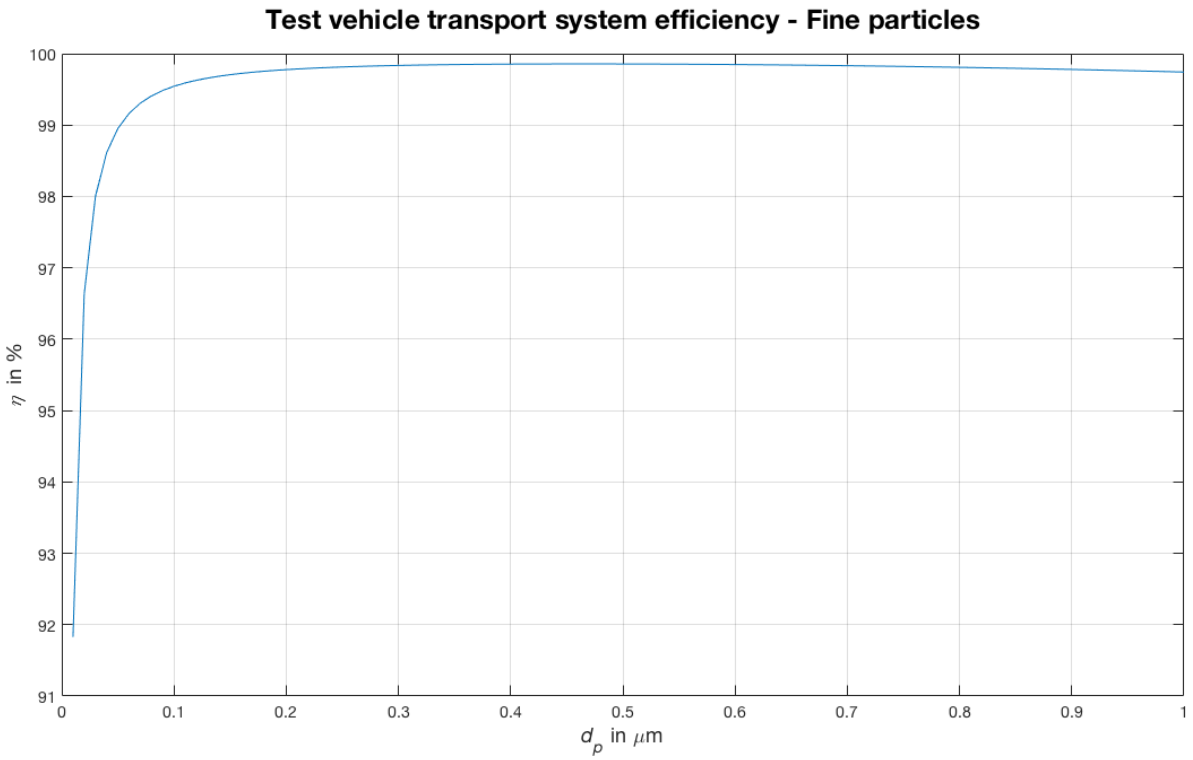

Figure 4.11: Graphic of test vehicle transport system (Fine particles)

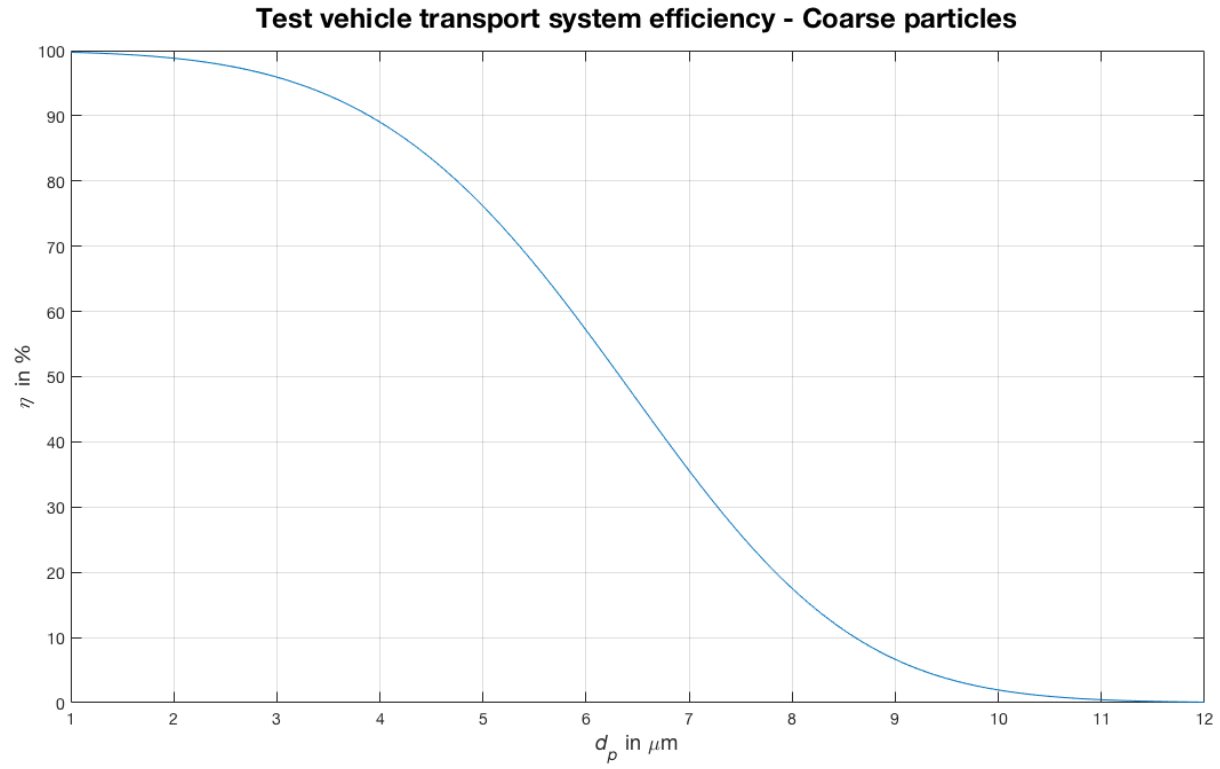

Figure 4.12: Graphic of test vehicle transport system (Coarse particles)

For particles in the submicron range, efficiency remains over 99% up to 100 nm of diameter. Then, it drops sharply. This is due to Brownian motion that affects small particles. As can be seen in the Table 4.5, efficiency in section 1, because of its length, is quite lower than in the rest of the sections for particles of 10 nm of diameter. In short, efficiency for fine particles larger than 100 nm is quite high and stable.

For particles larger than a micrometer, losses are less than 10% up to about 4 μm of diameter. For bigger particles, efficiency decreases being close to 0% for particles larger than 10 μm. That phenomenon is due, to a large extent, to the low efficiency for large particles in the sections 2, 4 and 6. Bends are located in these sections and, as has been observed in the previous section, a high number of big particles is lost in bends by inertial deposition in the walls of the tubes because of their weight and inertia.

After observing these results, the sparse number of big particles in the tests could be related the low efficiency of large particles in the transport system.

Particle diameter (μm)	Section 1	Section 2	Section 3	Section 4	Section 5	Section 6	TOTAL
0,01	96,9598	99,0931	98,7782	99,3383	98,4720	98,9123	91,8282
0,1	99,8317	99,9519	99,9350	99,9649	99,9175	99,9422	99,5440
0,25	99,9261	99,9819	99,9756	99,9868	99,9654	99,9782	99,8141
0,3	99,9319	99,9847	99,9795	99,9888	99,9688	99,9816	99,8355
0,38	99,9343	99,9875	99,9834	99,9909	99,9712	99,9850	99,8524
0,54	99,9254	99,9902	99,9877	99,9929	99,9699	99,9881	99,8542
0,78	99,8926	99,9900	99,9908	99,9929	99,9600	99,9876	99,8142
1,05	99,8356	99,9839	99,9927	99,9889	99,9415	99,9792	99,7220
1,34	99,7538	99,9658	99,9939	99,9769	99,9142	99,9550	99,5603
1,59	99,6670	99,9352	99,9946	99,9565	99,8850	99,9141	99,3540
2,07	99,4596	99,8117	99,9956	99,8742	99,8149	99,7494	98,7115
3	98,9082	99,1107	99,9966	99,4061	99,6275	98,8164	95,9310
4	98,1001	97,0290	99,9972	98,0092	99,3514	96,0586	89,0300
5	97,0741	92,5321	99,9976	94,9572	98,9991	90,1691	76,1382
6,5	95,1376	79,1056	99,9980	85,5338	98,3297	73,1606	46,3075
8	92,7407	57,8614	99,9983	69,4372	97,4939	48,2154	17,5149
10	88,8639	28,4086	99,9985	43,2149	96,1262	18,6753	1,9584
12	84,2577	10,4476	99,9987	22,1825	94,4764	4,9206	0,0908

Table 4.5: Table of efficiency in test vehicle transport system

5 Overall conclusions

The aim of this Bachelor thesis was to develop new approaches for measurements in real-drives. For this reason, two concepts have been developed and a study of the losses has been done to optimize the transport of particles samples.

The first approach, consisting of a full enclosure device, brings the opportunity to sample particulate matter emitted directly by the brake. This completely sealed device minimizes the losses by not letting particles entering or leaving the collecting box. By sealing the enclosure device in an ideal way, the results should be similar to those obtained in the IUTA dynamometer test stand since the flow conditions are conditioned by the enclosure device and the applied flow stream by the pump. For that reason, this concept has been rejected and a second approach, involving a rim shell device has been developed. The second concept permits the achievement of more realistic behavior of the particles emitted by the brake inside the rim. This is possible due to the flow entering through the air scoop and the interaction of the particles with the rim surface. Nevertheless, the turbulent flow inside the rim makes difficult to take representative particle samples. This fact and the limited time to manufacture and assembly the setup have been decisive to discard its construction during this Bachelor thesis. However, the next steps in the investigation of brake particles emissions have to be posed and this and other methods should be considered.

Regarding the study of transport losses, it has been observed that the most percentage of losses occurs to coarse particles due to their weight and inertia. Diffusional deposition losses affect small particles and losses are minimal (less than 1%) for particles larger than 100 nm. They only can be reduced by decreasing the tube length. Gravitational settling deposition losses in horizontal and inclined tubes affect large particles. Horizontal lines must be avoided and big angles of inclination, or vertical tubes, must be used to reduce this type of losses. Fine particles are almost not affected by inertial deposition in bends, and its losses can be negligible, but when the particle size increases the efficiency drops heavily. With the results obtained in this Bachelor thesis can be concluded that losses in the transport of particles must be taken into account, especially for coarse particles, and sampling lines can be optimized basically by:

1. Avoiding bends with small angles
2. Reducing tube length
3. Avoiding horizontal sections

For future works, experimental tests to corroborate the validity of the theoretical results can be done. Also, studying other mechanism of losses, such as losses in sampling inlets or in turbulent flow, could be useful for the optimization of aerosol transport.

Bibliography

Augsburg, K. et al.: Characterization of particulate emissions (2011)
Augsburg, K.; Horn, R.; Sachse, H.: Characterization of particulate emissions of vehicle wheel brakes, in: 56TH INTERNATIONAL SCIENTIFIC COLLOQUIUM, pp. 1–9, 2011

Augsburg, K. et al.: Measuring and characterization of brake dust particles (2017)
Augsburg, Klaus; Hesse, David; Wenzel, Felix; Eichner, Georg; Technische Universität Ilmenau, Germany; BMW AG, Germany: Measuring and characterization of brake dust particles, in: , pp. 1–15, 2017

Baron, P. A. et al.: Aerosol measurement (2011)
Baron, Paul A.; Kulkarni, Pramod; Willeke, Klaus: Aerosol measurement, in: , pp. 1–887, 2011

Giechaskiel, B. et al.: Sampling of Non-Volatile Vehicle Exhaust Particles (2012)
Giechaskiel, Barouch; Arndt, Michael; Schindler, Wolfgang; Bergmann, Alexander; Silvis, William; Drossinos, Yannis: Sampling of Non-Volatile Vehicle Exhaust Particles: A Simplified Guide, in: SAE International Journal of Engines (2), Issues 5, pp. 1–22, 2012

Gregory D. Wight: Fundamentals of air sampling (1994)
Gregory D. Wight: Fundamentals of air sampling, Lewis publishers, 1994

Grigoratos, T.; Martini, G.: Brake wear particle emissions (2015)
Grigoratos, Theodoros; Martini, Giorgio: Brake wear particle emissions: a review, in: Environmental science and pollution research international (4), Issues 22, pp. 2491–2504, 2015

Körner, M. et al.: Untersuchung der Bremsscheibenumströmung an einem Windkanalmodell (2007)
Körner, M.; Decker, F.; Dreyer, M.; Radespiel, R.: Untersuchung der Bremsscheibenumströmung an einem Windkanalmodell des VW Phaeton mit durchsichtigem Vorderrad, in: XXXIV. Internationales My-Symposium Bremsen-Fachtagung, pp. 2–27, 2007

Kukutschová, J. et al.: Wear performance and wear debris (2010)
Kukutschová, Jana; Roubíček, Václav; Mašláň, Miroslav; Jančík, Dalibor; Slovák, Václav; Malachová, Kateřina; Pavlíčková, Zuzana; Filip, Peter: Wear performance and wear debris of semimetallic automotive brake materials, in: Wear 1-2, Issues 268, pp. 86–93, 2010

Kukutschová, J. et al.: On airborne nano/micro-sized wear particles (2011)
Kukutschová, Jana; Moravec, Pavel; Tomášek, Vladimír; Matějka, Vlastimil; Smolík, Jiří; Schwarz, Jaroslav; Seidlerová, Jana; Safářová, Klára; Filip, Peter: On airborne nano/micro-sized wear particles released from low-metallic automotive brakes, in: Environmental pollution (Barking, Essex : 1987) (4), Issues 159, pp. 998–1006, 2011

Mathissen, M. et al.: Investigation on the potential generation of ultrafine particles (2011)
Mathissen, Marcel; Scheer, Volker; Vogt, Rainer; Benter, Thorsten: Investigation on the potential generation of ultrafine particles from the tire–road interface, in: Atmospheric Environment (34), Issues 45, pp. 6172–6179, 2011

McQuillan, F. J. et al.: Properties of dry air (1984)
McQuillan, F. J.; Culham, J. R.; Yovanovich, M. M.: Properties of dry air at one atmosphere, in: , pp. 1–5, 1984

Palas GmbH: DEHS properties
Palas GmbH: DEHS properties; https://www.palas.de/en/product/dehs

Pui, D. Y. et al.: Particle Deposition in Bends (1987)
Pui, David Y. H.; Romay-Novas, Francisco; Liu, Benjamin Y. H.: Experimental Study of Particle Deposition in Bends of Circular Cross Section, in: Aerosol Science and Technology (3), Issues 7, pp. 301–315, 1987

Sachse, H.; Augsburg, K.: Study on Appropriate Measurement Methods (2015)
Sachse, Hannes; Augsburg, Klaus: Study on Appropriate Measurement Methods and Test Procedures for Assesment of Brake-induced Emissions, in: XXXIV. Internationales My-Symposium Bremsen-Fachtagung, pp. 134–160, 2015

Sanders, P. G. et al.: Brake Dynamometer Measurement (2002)
Sanders, P. G.; Dalka T.M.; Xu, N. Maricq, M.M.; Basch, R. H.: Brake Dynamometer Measurement of Airborne Brake Wear Debris, in: Society of Automotive Engineers, Inc., pp. 1–9, 2002

Sanders, P. G. et al.: Airborne Brake Wear Debris (2003)
Sanders, P. G.; Xu, N.; Dalka, Tom M.; Maricq, M. M.: Airborne Brake Wear Debris: Size Distributions, Composition, and a Comparison of Dynamometer and Vehicle Tests, in: Environmental Science & Technology (18), Issues 37, pp. 4060–4069, 2003

Söderberg, A. et al.: A Pin on Disc Simulation (2008)
Söderberg, Anders; Wahlström, Jens; Olander, Lars; Jansson, Anders; Olofsson; Ulf: On Airborne Wear Particles Emissions of Commercial Disc Brake Materials - A Pin on Disc Simulation, in: Department of Machine Design Royal Institute of Technology SE-100 44 Stockholm, pp. 1–54, 2008

The University of Manchester: Aerodynamic Particle Sizer
The University of Manchester - Centre for Atmospheric Science: Aerodynamic Particle Sizer; http://www.cas.manchester.ac.uk/restools/instruments/aerosol/aps/, 8.8.2018

The University of Manchester: Impactors and Filters
The University of Manchester - Centre for Atmospheric Science: Impactors and Filters; http://www.cas.manchester.ac.uk/restools/instruments/aerosol/impactors/, 8.8.2018

The University of Manchester: Optical Particle Counters
The University of Manchester - Centre for Atmospheric Science: Optical Particle Counters; http://www.cas.manchester.ac.uk/restools/instruments/aerosol/opc/, 6.8.2018

TSI Incorporated Ltd: Model 3321 (2004)
TSI Incorporated Ltd: Model 3321 Aerodynamic Particle Sizer Spectrometer, 2004

TSI Incorporated Ltd: Model 3007 (2012)
TSI Incorporated Ltd: Hand-held condensation Particle Counter Model 3007, 2012

TSI Incorporated Ltd: Model 3330 (2012)
TSI Incorporated Ltd: Optical Particle Sizer Model 3330, 2012

Wahlström, J. et al.: A disc brake test stand (2009)
Wahlström, Jens; Söderberg, Anders; Olander, Lars; Olofsson, Ulf: A disc brake test stand for measurement of airborne wear particles, in: Lubrication Science (6), Issues 21, pp. 241–252, 2009

Wahlström, J. et al.: Airborne wear particles from passenger car disc brakes (2010)
Wahlström, J.; Söderberg, A.; Olander, L.; Olofsson, U.; Jansson, A.: Airborne wear particles from passenger car disc brakes: A comparison of measurements from field tests, a disc brake assembly test stand, and a pin-on-disc machine, in: Proceedings of the Institution of Mechanical Engineers, Part J: Journal of Engineering Tribology (2), Issues 224, pp. 179–188, 2010

Wahlström, J.; Olofsson, U.: A field study of airborne particle emissions (2015)
Wahlström, Jens; Olofsson, Ulf: A field study of airborne particle emissions from automotive disc brakes, in: Proceedings of the Institution of Mechanical Engineers, Part D: Journal of Automobile Engineering (6), Issues 229, pp. 747–757, 2015

Weiden, S.-L. von der et al.: Particle Loss Calculator (2009)
Weiden, S.-L. von der; Drewnick, F.; Borrmann, S.: Particle Loss Calculator – a new software tool for the assessment of the performance of aerosol inlet systems, in: Atmospheric Measurement Techniques (2), Issues 2, pp. 479–494, 2009